POLARIZATION AT POROUS FLOW-THROUGH ELECTRODES

L. G. Austin, P. Palasi and R. R. Klimpel
Fuel Technology Department, Pennsylvania State University,
University Park, Pa.

INTRODUCTION

The flow-through electrode is an electrochemical system which has received little attention. It is of primary interest in redox fuel cells (1, 2, 3) where a dissolved ionic fuel (or oxidant) is to be reacted at an electrode. In such a system, where liquid is circulated through the cell, it is clearly much better to force the fresh liquid through the electrode and take spent liquid from the exit side. The electrode then acts as a separator between fresh and spent liquid and, more important, the mass transport of reactant to the electrode can be easily controlled. By forcing electrolyte through the electrode, we no longer have to rely on diffusion of fuel to the electrode and, consequently, the mass transport problems of non flow-through electrodes can be considerably diminished. Similarly, for fuels or oxidants such as methanol, hydrazine, nitric acid, etc., which can be dissolved in high concentrations in the electrolyte, it may be desirable to use flow-through electrodes (4, 5, 6).

When the processes occuring in flow-through electrodes are considered, it readily becomes apparent that several parameters are of first importance. The concentration of reactant and rate of flow determine the maximum current which can be drawn, since we cannot draw more current than the corresponding amount of reactant put in per second. The speed of the electrochemical reaction, in the form of the exchange current for the reaction (7), is of importance in determining the polarization at a given current. In addition, the ohmic voltage gradient in the electrolyte in the pores of the electrode also affects the polarization.

Perskaya and Zaidenman (8) gave the basic mathematical form of the process. However, they solved the equation only for low current density, low polarization conditions, where the approximation $\exp(\alpha n F\eta/RT) = 1 + \alpha n F\eta/RT$ applies. In our analysis we have found that this can only rarely be applied. The treatment we give explains reasonably well the whole current-voltage range of their experimental results and also explains the experimental results of Bond and Singman (9). However, the assumptions made in the theory are not generally valid and the breakdown of the theory is demonstrated and discussed.

PHYSICAL SYSTEM TREATED AND ASSUMPTIONS INVOLVED.

The physical system studied consists of a uniform, porous, plane electrode with reactant dissolved in electrolyte flowing into the left hand face; unreacted reactant and dissolved product flow out of the right hand face (see Figure 1). The reaction could be a simple redox reaction such as $Fe^{2+} \rightleftarrows Fe^{3+} + e$ in acid solution. In a redox cell employing a separator the circuit is completed within the cell by (H^+) flowing from the anode to the cathode. The following assumptions are made. (i) The flow is uniform through the electrode. This is very nearly true for a small experimental electrode, but it may not be so for a large electrode. (ii) Ohmic loss in the material of the electrode is negligible. This will be a good approximation for properly constructed electrodes of metal or carbon. (iii) The reaction at the external faces of the electrode is small compared to the total reaction. The external faces can be considered as extensions of the internal area and the assumption would only be false in the limit where the internal area became

small. (iv) The pores of the electrode are small in radius compared to their length, so that negligible concentration gradients exist across the radius of the pore. In other words, the pore radius is so small that radial diffusion is rapid enough to maintain uniform concentration across the pore radius; the only concentration changes will be linear along the axis of the pore. With this assumption, the variation of laminar flow rate across the pore radius is of no consequence. This assumption is discussed later in more detail. (v) The porous electrode has its pores so well interlinked that it can be considered to act as a homogenous system, with variation of conditions at a given penetration applying only over small regions. Electrodes must be constructed so that no major cracks or pinholes exist. (vi) The flow rate is great enough that axial mass transfer of reactant and product by diffusion and ionic migration is negligible compared to mass transfer by the bulk flow. It should be noted that the current must be supported by ionic migration and, therefore, this assumption may not always be valid. It will be a good approximation, however, when the concentration of supporting electrolyte is high, e.g. a strongly acid solution is used. In this case we can also assume that the specific conductivity of the electrolyte remains constant. (vii) The streaming potential is small compared to other effects, which will be true when strong electrolytes are used.

A less easily justified assumption is that the electrochemical reaction at the pore surface is a simple reaction with the rate form (7)

$$i = i_o[(R/R_i)e^{\eta/b} - (P/P_i)e^{-\eta/b}] \qquad (1)$$

R_i, P_i are the entering concentrations (assumed equivalent to activities) of the reactant and product; i, i_o refer to unit area of the pore surface, (see list of nomenclature). Equation 1 may apply to simple redox reactions, but one would expect, for example, dissolved methyl alcohol fuel to have a more complex form. At open circuit conditions, with no current flow, R and P are constant though the electrode and equal to R_i and P_i, and they determine the theoretical potential. However, if the basic exchange current is small then impurities in the feed may give rise to leakage current and a mixed potential may be obtained. A sufficient rate of flow will prevent diffusion of a disturbing material from the other electrode, but any impurities in the feed are being constantly replaced. Thus, very low current density measurements and open circuit potentials may not correspond to ideal values.

THEORY

Consider unit face area of the electrode. Let the velocity of flow through the electrode be v, cm^3 per sq cm of face per second. Consider element dx in Figure 1. The amount of reactant flowing in per second is Rv and the amount flowing out is $[R + (dR/dx)dx]v$. The amount of R reacted to P in the element, per second, is given by

$$di/nF = i_o[(R/R_i)e^{\eta/b} - (P/P_i)e^{-\eta/b}](S/nF)dx \qquad (2)$$

n is the total number of electrons involved for each complete reaction; S is the reacting area per unit volume of electrode. At steady state, therefore,

$$Rv - [R + (dR/dx)dx]v = (i_oS/nF)[(R/R_i)e^{\eta/b} - (P/P_i)e^{-\eta/b}]dx$$

or

$$-dR/dx = (i_oS/vnF)[(R/R_i)e^{\eta/b} - (P/P_i)e^{-\eta/b}] \qquad (3)$$

Also, at steady state, $R_i + P_i = R + P$, therefore

$$-dR/dx = (i_oS/vnF)[R\left(\frac{e^{\eta/b}}{R_i} + \frac{e^{-\eta/b}}{P_i}\right) - \frac{(R_i + P_i)}{P_i}e^{-\eta/b}] \qquad (4)$$

If the specific resistance of the electrolyte is ρ', the porosity of the electrode

ϵ and the tortuosity factor q (10) then, by Ohm's law,

$$(\rho' q/\epsilon) i = d\eta/dx$$

or

$$i = (1/\rho)\, d\eta/dx \qquad (5)$$

where ρ is understood to include the porosity and tortuosity factors.

The complete solution to the problem is given by the solution of equations 4 and 5. We could not, however, obtain an analytical solution. Computed results are presented later, but it is informative to consider a limiting condition which has an analytical solution. The limiting condition is that the ohmic drop within the electrolyte in the pores is negligible. The effect of ohmic drop can be considered as a disturbance of this limiting condition.

CASE 1. Ohmic Effects Neglected

Neglecting ohmic drop and working with equation 4 only, we can separate and integrate from $x = 0$, $R = R_i$ to $x = x$, $R = R$,

$$(i_o S/vnF)x = \frac{1}{((e^{\eta/b}/R_i) + (e^{-\eta/b}/P_i))} \ln\left[\frac{(e^{\eta/b} - e^{-\eta/b})}{(R/R_i)e^{\eta/b} - ((R_i + P_i - R)/P_i)e^{-\eta/b}}\right] \qquad (6)$$

When $x = L$, the thickness of the electrode, $R = R_f$, the final concentration of reactant issuing from the right hand face of the electrode. The current per sq cm of electrode is

$$i = nFv(R_i - R_f) \qquad (7)$$

The limiting current density is clearly given by

$$i_L = nFvR_i \qquad (7a)$$

Thus

$$i/i_L = 1 - R_f/R_i = \text{degree of conversion} \qquad (8)$$

To get the relation between current and polarization we have to substitute for R_f in equation 6 using equation 8, as follows

$$(Li_oS/vnF)((e^{\eta/b}/R_i) + (e^{-\eta/b}/P_i))$$
$$= \ln(e^{\bar{\eta}/b} - e^{-\bar{\eta}/b}) - \ln[(R_f/R_i)e^{\bar{\eta}/b} - (R_i/P_i)e^{-\bar{\eta}/b} - e^{-\bar{\eta}/b} + (R_f/P_i)e^{-\bar{\eta}/b}]$$

For algebraic convenience let $\gamma = R_i/P_i$, $Q = e^{\eta/b} - e^{-\eta/b}$, then

$$(Li_oS/vnFR_i)(e^{\eta/b} + \gamma e^{-\eta/b})$$
$$= \ln Q - \ln[(R_f/R_i)(e^{\eta/b} + e^{-\eta/b}) - (1 + \gamma)e^{-\eta/b}]$$

Again, for algebraic convenience let $e^{\eta/b} + \gamma e^{-\eta/b} = f$, then

$$e^{-(Li_oS/i_L)f} Q = (R_f/R_i)f - (1 + \gamma)e^{-\eta/b}$$

$$\text{or } i/i_L = 1 - R_f/R_i = (f - Qe^{-(LSi_o/i_L)}f - (1 + \gamma)e^{\gamma\eta/b})/f$$
$$= (e^{\eta/b} + \gamma e^{-\eta/b} - e^{-\eta/b} - \gamma e^{-\eta/b} - Qe^{-(LSi_o/i_L)f})/f$$

$$\text{or } i/i_L = Q\,(1 - e^{-(LSi_o/i_L)f})/f \qquad (9)$$

This is the equation relating current to polarization and it includes the parameters of i_o, S, L, v, R_i, P_i.

Two limiting cases can be considered. Firstly, let us consider the low current case where $\eta \to 0$.
Using $e^{\eta/b} = 1 + \eta/b$ when η/b is small,

$$i/i_L = \frac{2(\eta/b)}{1 + \frac{\eta}{b} + \gamma\left(1 - \frac{\eta}{b}\right)}\left(1 - e^{-(LSi_o/i_L)\left[1 + \frac{\eta}{b} + \gamma\left(1 - \frac{\eta}{b}\right)\right]}\right)$$

When LSi_o/i_L is small, that is, it is a reaction with a relatively low exchange current,

$$i/i_L = 2(LSi_o/i_L)(\eta/b) \qquad (10)$$

This is the required logical result since, as $b = RT/\alpha n_1 F$, $\alpha \sim 1/2$ (n_1 is the electron transfer in the rate controlling step),

$$i = (LSi_o)n_1 F\eta/RT \ .$$

On the other hand, if LSi_o/i_L is large, then

$$i/i_L = Q/f$$
$$= (e^{\eta/b} - e^{\eta/b})/(e^{\eta/b} + \gamma e^{-\eta/b}) .$$

Rearranging

$$\eta = (2.3RT/nF)\ \log\left[\frac{(1 + \gamma i/i_L)}{(1 - i/i_L)}\right] \qquad (11)$$

This is again the expected result: it corresponds to pure concentration polarization (see reference 7, p. 15, where the above result can be obtained from equation 26a by setting $i/I = 0$).

At large values of η (the larger is γ the larger η must be for the following approximation to hold) $e^{-\eta/b}$ can be neglected compared to $e^{\eta/b}$ and

$$i/i_L = 1 - e^{-(SLi_o/i_L)\ e^{\eta/b}} \qquad (12)$$

As necessary, as η/b becomes large, $i/i_L \to 1$. Figure 2 shows the form of i versus η for various values of exchange current. To make the curves as general as possible it is convenient to plot in the form i/i_L versus η/b, with $\bar{i}_o/i_L$ as the variable parameter. $\bar{i}_o$ is defined by

$$\bar{i}_o = i_o SL \ . \qquad (13)$$

For small values of $\bar{i}_o/i_L$, the electrode is highly polarized and the factor $\gamma(=R_i/P_i)$ does not affect the result. A Tafel region is observed at current densities well below the limiting current. This can be predicted from equation 12, since when i/i_L is less than 0.1, the exponential term is near 1 and

$$i/i_L \simeq (\bar{i}_o/i_L)\ e^{\eta/b}$$
$$\eta \simeq (2.3RT/\alpha n_1 F)\ \log(i/\bar{i}_o) \qquad (12a)$$

CASE 2. Ohmic Effects Included

From equation 5 we have

$$di/dx = (1/\rho)\ d^2\eta/dx^2 \ .$$

From equation 7 we have

$$di/dx = -vnF\ dR/dx \ .$$

We can also combine equations 5, 7 and 7a to give

$$R/R_i = (1 - (1/i_L\rho)d\eta/dx) \ .$$

Combining these equations with equation 4 gives

$$d^2\eta/dx^2 = \rho i_o S\left[R_i\left(1 - \frac{1}{i_L\rho}\frac{d\eta}{dx}\right)\left(\frac{e^{-\eta/b}}{R_i} + \frac{e^{-\eta/b}}{P_i}\right) - \frac{(R_i + P_i)e^{-\eta/b}}{P_i}\right] . \qquad (14)$$

Equation 14 is the basic equation relating polarization to distance into the electrode. We were not able to find a general analytical solution to the equation,

therefore, the equation was put into a form suitable for numerical integration.

For computational convenience it is helpful to define reduced values of η, x by

$$\bar{\eta} = \eta/b \tag{15}$$

$$\bar{x} = x/L \tag{15a}$$

It is also convenient to define a maximum ohmic polarization Δ by

$$\Delta = i_L \rho L \tag{16}$$

Δ is the maximum possible ohmic loss through the electrode and is obtained under conditions where the reaction is completed in a differential element at x = 0, so that all the ions supporting i_L have to be transported from L to x = 0 (or x = 0 to L). This can only occur at very large total polarizations. Replacing R_i/P_i by γ, η/b by $\bar{\eta}$, and x/L by $\bar{x}$, equation 14 goes to

$$d^2\bar{\eta}/d\bar{x}^2 = (\bar{i}_o/i_L)(\Delta/b)\left[\left(1-\frac{b}{\Delta}\frac{d\bar{\eta}}{d\bar{x}}\right)(e^{\bar{\eta}} + \gamma e^{-\bar{\eta}}) - (1+\gamma)e^{-\bar{\eta}}\right] .$$

Again, it is convenient to define a reduced Δ by

$$\bar{\Delta} = \Delta/b \ . \tag{16a}$$

Then, dropping the bar but remembering that i_o, η and Δ are reduced quantities,

$$d^2\eta/dx^2 = (i_o/i_L)\ \Delta[(1-(1/\Delta)d\eta/dx)(e^{\eta}+\gamma e^{-\eta}) - (1+\gamma)e^{-\eta}] .$$

The boundary conditions are $\eta = \eta_o$ at x = 0 and $\eta = \eta_L$ at x = 1, where η_L is the polarization at the right hand face of the electrode in multiples of b. Integrating equation 17 once,

$$d\eta/dx = (i_o/i_L)\left[\Delta\int_{\eta_o}^{\eta}(e^{\eta} + \gamma e^{-\eta} - e^{-\eta} - \gamma e^{-\eta})dx - \int_{\eta_o}^{\eta}(e^{\eta} + \gamma e^{-\eta})d\eta\right]$$

$$= (i_o/i_L)\left[\Delta\int(e^{\eta} - e^{-\eta})dx - ((e^{\eta} - \gamma e^{-\eta}) - (e^{\eta_o} - \gamma e^{-\eta_o}))\right]$$

If x is divided into M small increments of Δx such that over any Δx, η is proportional to x and $\Delta\eta/\Delta x$ is a constant we get, at the N'th increment,

$$\Delta\eta_N = (i_o/i_L)\Delta x \left(\lim_{(\Delta x \to 0)}\ \Delta\sum_1^N (\Delta x/\Delta\eta_N)[(e^{\eta_N} + e^{-\eta_N}) - (e^{\eta_{N-1}} + e^{-\eta_{N-1}})]\right.$$

$$\left. -[(e^{\eta_N} - \gamma e^{-\eta_N}) - (e^{\eta_o} - \gamma e^{\eta_o})]\right) \tag{18}$$ *

$\Delta\eta_N$ is the increase in polarization over the N-1 to N^{th} increment. Also, from equation 5,

$$i/i_L = (1/\rho i_L)\ d\eta/dx$$

where η, x are actual values. Replacing, as before, η/b with $\bar{\eta}$, x/L with $\bar{x}$

$$i/i_L = (b/\rho i_L L)\ d\bar{\eta}/d\bar{x} = (1/\bar{\Delta})d\bar{\eta}/d\bar{x} .$$

Dropping the bars,

$$i/i_L = (1/\Delta)\ d\eta/dx .$$

Thus the total current density from the electrode is

$$i/i_L = (1/\Delta)\ (d\eta/dx)_{x\,=\,1} \tag{19}$$

To calculate η and i/i_L, equation 18 is progressively solved using a suitable value of Δx and the value of η plotted versus x. The value of $d\eta/dx$ at x = 1 is obtained graphically. Equation 18 is solved by assigning a value of η_o and guessing at a value of $\Delta\eta_1$. This is substituted into the R.H.S. of equation 18, with $\eta_1 = \eta_o + \Delta\eta_1$. $\Delta\eta_1$ is calculated. When it agrees with the substituted value of $\Delta\eta_1$ within a specified error, the calculation is correct and may proceed to the

* The program for computation of equation 18 is available from the authors.

next step. The final polarization is at x = 1, N = M, and the total current is obtained from equation 19. This is repeated for another value of η_o (which is the polarization at the left hand face of the electrode) and other values of η (at the right hand face) and i/i_L are obtained. By this means, the complete range of η_o, η and i/i_L, from i/i_L small to $i/i_L \to 1$ can be obtained. For $\gamma \leq 1$, terms in $e^{-\eta}$ can be neglected when η_o is greater than 1, and equation 18 goes to

$$\Delta\eta_N \simeq (i_o/i_L)\Delta x e^{\eta_o}[\Sigma\Delta(\Delta x/\Delta\eta_N)(e^{\eta^1_N} - e^{\eta^1_{N-1}}) - (e^{\eta^1_N} - 1)] \qquad (20)$$

where η^1 is measured from η_o, that is, $\eta = \eta^1 + \eta_o$. This form can be fairly rapidly computed. When $(i_o/i_L)(\Delta x)e^{\eta_o\Delta}$ is small, the final value of η^1 is small and

$$\begin{aligned} d\eta/dx &= (i_o/i_L)\, e^{\eta_o\Delta\Sigma}\, \frac{\Delta x}{\Delta\eta}(1 + \eta_N - 1 - \eta_{N-1}) \\ &= (i_o/i_L)\, e^{\eta_o\Delta\Sigma\Delta x} \\ &= (i_o/i_L)\Delta e^{\eta_o x} \end{aligned}$$

Therefore,

$$\begin{aligned} \eta^1_x &= (i_o/i_L)e^{\eta_o\Delta}\int^x x\, dx \\ &= (i_o/i_L)\Delta e^{\eta_o x^2_o/2} \end{aligned} \qquad (21)$$

For this low current condition

$$\begin{aligned} i/i_L &= (1/\Delta)(d\eta/dx)_{x=1} = (1/\Delta)(i_o/i_L)e^{\eta_o\Delta} \\ &= (i_o/i_L)e^{\eta_o} \end{aligned} \qquad (22)$$

This, of course, is a Tafel form. The equations tell us that, for an irreversible reaction at low current, the additional polarization η^1 caused by ohmic loss is one-half that expected if all of the current flowed completely through the porous system, since, from equation 21

$$\begin{aligned} \eta^1_{x=1} &= (i_o/i_L)e^{\eta_o\Delta/2} \\ &= (i/i_L)\Delta/2 \end{aligned}$$

This is reasonable, since, under these conditions, the electrode is reacting uniformly throughout its thickness and the mean distance the ions have to penetrate is half the thickness.

Equation 20 predicts that, for irreversible conditions, the shape of the η versus i/i_L curves will be the same for any i_o/i_L value (for a given Δ value, of course) but shifted to higher or lower polarizations. This is because $(i_o/i_L)e^{\eta_o}$ is the controlling parameter and we therefore know that η^1 is the same for a given value of $(i_o/i_L)e^{\eta_o}$. Thus for a given set of η^1 values

$$(i_o/i_L)_1 e^{\eta_o} = (i_o/i_L)_2 e^{(\eta_o + \Delta\eta_{12})}$$

where $\Delta\eta_{12}$ represents the bodily shift. Then

$$\Delta\eta_{12} = 2.3\, \log[(i_o/i_L)_1/(i_o/i_L)_2]$$

or

$$\Delta\eta_{12}\text{volts} = (2.3b)\ \log[(i_o/i_L)_1/(i_o/i_L)_2]$$

Let us now consider the limiting case where activation polarization is negligible and only concentration and ohmic effects are present. From equation 17, when $(i_o/i_L)\Delta$ is large, $d^2\eta/dx^2/(i_o/i_L)\Delta$ tends to zero and we get equation 11. Equation 11 thus represents the limiting case whether an internal ohmic voltage gradient is present or not. For a given η_o, a larger ohmic effect will give a higher i/i_L since the concentration of reactant and product will change to keep match with the voltage: but since η_o is essentially zero at all currents up to near the limiting current, η is determined solely by i/i_L, according to equation 11. The position of reaction in the interior will change with Δ, but the final result will not.

At intermediate conditions where neither equation 20 nor equation 11 apply, equation 18 is tedious to compute. However, if $\gamma = 1$ the equation goes to

$$\Delta\eta_N = (2i_o/i_L)\Delta x[\Sigma_1^N\Delta \frac{\Delta x}{\Delta\eta}(\cosh\eta_N - \cosh\eta_{N-1}) - (\sinh\eta_N - \sinh\eta_o] \qquad (18a)$$

Tables of hyperbolic functions can then be used.

RESULTS OF COMPUTATIONS

In a previous report (11), the equations were solved by hand computation. They have since been solved more accurately on an IBM 7074 digital computer. The later results show a slight change in the values of η_o as compared to the former. Figure 3, 4 and 5 show the results of computations of the full equation, allowing for ohmic resistance. (A value of $\Delta x = 1/20$ was found to be satisfactory over most of the current range.) To avoid confusion, the η calculated for the case of no ohmic effect is termed η_s, the polarization at the entering face is termed η_o and the polarization of practical importance, at the exit face, is termed η.

The physical picture of the effect of ohmic voltage gradient which emerges from the solution of the equations is as follows. The flowing electrolyte, with a high concentration of fuel, enters at one face and, with a suitable polarization, it starts to react. The ionic transfer through the electrolyte, which maintains charge balance, gives rise to an ohmic voltage gradient. This ohmic effect increases the polarization at further penetration into the electrode and the reaction rate is increased. Therefore, as the fuel flows through the electrode, it is consumed more and more rapidly, which increases the cumulative ion transfer, which causes increased ohmic effect, which increases the rate of consumption and so on. Thus for a large value of Δ (the index of ohmic effect) the reaction is concentrated towards the exit face of the electrode. This is shown in Figure 6 for $\Delta = 100$ and currents of 0.84 and 0.23 of the limiting current. For the larger value, most of the reaction occurs in the final one-tenth of the electrode. For the lower value, most of the reaction occurs in the final three-tenths. An important effect of this concentration of the reaction in a zone towards the exit face is that radial mass transfer limitations across the pore may come into play sooner than would be expected if reaction were more uniformly distributed through the pore.

The curves in Figure 3 are calculated for a Δ/b value of 10. Examining the curves for $\bar{i}_o/i_L = 10^{-2}$ it is seen that η_o and η lie on either side of the η_s curve. This is as expected, because the ohmic voltage gradient in the electrode speeds up the reaction toward the exit face, therefore, the initial activation polarization η_o, has to be less to give a certain i/i_L value. As predicted by equations 22 and 12a, the η_o value at low current density (but reaction still irreversible) approaches η_s, both being given by a Tafel form. At $i/i_L = 0.1$, $\eta-\eta_o \simeq 1/2b$. If this current flowed completely from the left hand face of the electrode, the ohmic drop would be $(i/i_L)\rho Li_L = (i/i_L)\Delta = (0.1)(10b)$. Thus the actual $\eta-\eta_o$ is one-half the maximum possible $\eta-\eta_o$, as predicted previously by equation 21. Over most of the current

density range of importance, i/i_L from 0.2 to 0.95 for example, the difference between η and η_s is less than 1/5 of the maximum possible ohmic effect. Again, this is reasonable, because the increase in polarization from entrance to exit in the electrode causes the reaction to proceed faster towards the exit. Therefore, the mean distance which the current carrying ions have to traverse is strongly weighted to be near the exit face, giving a relatively small ohmic drop. Of course, as the limiting current is approached very closely, all of the reaction occurs towards the entrace face giving the complete ohmic drop. This condition is only reached as the polarization becomes very large.

We can see, therefore, that the simpler analytical equations leading to Figure 2 are of value since they predict the main features of the process. The ohmic effect is a secondary effect. Both Figures 2 and 3 show that a decrease in the basic parameter $\bar{i}_o/i_L$ causes a bodily shift of the curves, with no difference in shape. Considering Figure 2, it can be seen that, as expected, decrease of $\bar{i}_o/i_L$ by a factor of 10 bodily shifts the polarization curve down by 2.3b volts. (The 2.3 arises because b is $RT/\alpha n_1 F$, whereas the normal Tafel coefficient is $2.3RT/\alpha n_1 F$.) For a one electron process at room temperature the shift would be about 0.12 volts, and for a two electron process, 0.06 volts.

In Figure 2, the uppermost curve represents equation 11 with $\gamma = 1$. This is a pure concentration polarization curve and applies for all values of $\bar{i}_o/i_L$ above about 1 or 2. The reaction is essentially reversible at all fractional current densities*. For the more polarized, irreversible curves, γ has no significance, but it has a large effect for the reversible case.

The effect of change of Δ is shown in Figure 4. The results were computed for $\Delta/b = 0$, 10, 20, 50 and 100. This covers most of the range likely to be encountered for electrodes of reasonable porosity and strongly conducting electrolytes. Figure 5 shows the polarization for a one electron rate controlling step at room temperature where the normal Tafel coefficient would be 0.12 volts. For a given limiting current (given by the flow rate and concentration of reactant), the important parameters are the effective exchange current $\bar{i}_o$, the effective ohmic resistance of the electrolyte in the pores and αn_1, determined principally by the number of electrons transferred in the rate controlling step. The ohmic effect, represented by Δ, does not give a linear effect on the polarization. For example, in going from $\Delta/b = 10$ to $\Delta/b = 50$, the difference between η and η_s over the practical range is not increased 5 times, but less than 5 times. Again, this is to be expected since the higher ohmic voltage gradient forces the reaction to occur at nearer the exit face.

Figure 7 shows the results plotted for limiting currents in the ratios 1:2:5, but with the same $\bar{i}_o$. This would correspond to a given electrode and fuel at different flow rates. Note that Δ/b will vary in the same ratio, while $\bar{i}_o/i_L$ will vary as the inverse of the ratio. Figure 7 shows that the initial portions of the curves are almost identical. The figure may be compared with the experimental results given later.

DATA FROM THE LITERATURE

The theory discussed above was first tested on two sets of experimental results taken from the literature. The first set (9) is shown in Table 1. The results for $i_L = 80$ m amps/cm^2 are plotted in Figure 8. Comparing with Figure 5 it can be seen that $i_o/i_L = 10^{-2}$, $\Delta/b = 20$, $\alpha n_1 = 1/2$, is one set of conditions that approximately fit the experimental results. The test of these values is whether they will accurately predict the polarization at the other limiting current

---

* It should be noted, however, that $\exp(\eta/b)$ cannot be set equal to $1 + \eta/b$ over all the range, because, although reversible, strong concentration polarization exists.

TABLE I

Polarization versus current for anodic reaction of Sn^{2+}/Sn^{4+} in a flow-through electrode of porous carbon (9)

Thickness of electrode	=	0.4cm
Feed concentration of Sn^{2+}	=	0.26 N
Feed concentration of Sn^{4+}	=	0.30 N
Electrolyte	=	6 N HCl
Temperature	=	23°C
Area of electrode	=	5 cm^2

	Expt A		B		C	
i m amps/cm	i_L ma/cm^2	η volts	i_L	η	i_L	η
10	80	0.17	150		400	
20		0.23				
30		0.27		0.265		
40	Flow 0.96 ml/min	0.31	Flow 1.80 ml/min	0.29	Flow 4.92 ml/min	0.30
50		0.34		0.315		
60		0.38		0.34		0.34
70		0.42		0.37		
80				0.39		0.375
90				0.41		
100				0.43		0.41
110				0.46		
120				0.50		0.435
140				0.65		0.465
160						0.485
180						0.51
200						0.53

densities. Thus, for i_L = 150 m amps/cm^2 i_o/i_L must be (80/150) 10^{-2} = (5.3) 10^{-3}, and Δ/b = (150/80) 20 = 38. For i_L = 400 m amps/cm^2, i_o/i_L = (2) 10^{-3}, Δ/b = 100. Figures 8a, 8b, 8c compare the predicted with the experimental values. Bearing in mind that the values of $i_o/i_L = 10^{-2}$, Δ/b = 20, αn_1 = 1/2 were obtained by visual comparison and are thus only estimations, the agreement between predicted and experimental results is good. Figure 8c also shows the predicted values of η_s, the activation-concentration polarization without ohmic effects.

If the value of Δ/b is 20 at i_L = 80 m amps/sq cm then the effective specific resistance ρ is given by

$$\Delta = i_L L\rho = 20b, \quad \rho = (20)(0.052)/(0.08)(0.4) \text{ ohm cm} = 32.5 \text{ ohm cm}.$$

The concentrated solutions used (6N HCl) should have a resistivity of about 2 therefore

$$\rho' = \rho(\epsilon/q) \simeq 2 \text{ or } \epsilon/q = 2/(32.5) = 1/16.$$

This value appears to be lower than the optimum, since we would expect ϵ/q to be about 1/5 for normal porosities and tortuosity coefficients. However, a tortuosity factor of 5 and a porosity of about 30% would give the required ϵ/q value, and tortuosity factors up to 5 or even much higher are often found in compacted bodies (10). Such high tortuosity factors can sometimes be lowered to more normal values of about $\sqrt{2}$ by burning out the carbon to remove constrictions and blockages in the structure.

The interesting question now arises as to why αn_1 = 1/2 gives reasonable values, when the over-all process is a two electron process. If αn_1 is set equal to 1, b is 0.026. This means that the predicted polarization due to activation - concentration effects at any given i/i_L is very much reduced and more of the actual polarization must be ascribed to ohmic loss. The values of Δ/b (and hence q/ϵ) become much greater; the values of i_o and Δ obtained using one set of experimental results do not give predictions which fit the other two sets of experiment results. There is strong evidence, therefore, that the $Sn^{2+} \rightarrow Sn^{4+}$ reaction has a one electron rate controlling step. An explanation for this has been given by Vetter (12).

i_o/i_L for a limiting current of 80 m amps/sq cm is 10^{-2}, therefore, the exchange current for the carbon electrode is 0.80 m amps/sq cm. Since the thickness of electrode is 0.4 cms, the exchange current per cubic cm of electrode is 2 m amps. As the internal area of the carbon electrode is now known it is not possible to convert this figure to a true exchange current per unit area. It must be recognized that the absence of data on η_o values makes the treatment somewhat conjectural.

The second set of experimental results obtained from the literature are those of Perskaya and Zaidenman (8). These authors give essentially the same equation as equation 14, but they solved it (analytically) only for a short range of current density, for low polarization conditions. The analytical form is too complex to be of much use. In one experiment, however, they measured η_o and η. They used a 1 mm thick disc of porous platinum prepared from platinum powder and the reaction studied was $Fe^{2+} \rightarrow Fe^{3+}$, at equal inlet concentrations of 0.005 N in 1 N H_2SO_4. Figure 9 shows their results in terms of η versus i/i_L, for a limiting current of about 180 m amps/sq cm. These results may be compared to the shape of the η, η_o curves computed for i_o/i_L = 0.5 and Δ/b = 5, also shown in Figure 9 (if αn_1 is 1/2, the scales of the two figures are identical). The two curves have a strong resemblance and adjustment of αn_1, i_o/i_L and Δ/b could no doubt be made to bring the η values into better correspondence. The η_o values, however, appear to be too different to correct by such an adjustment, since the experimental values approach the limiting current more gradually than predicted. This may be due to assumption

iv being false near the limiting current, (see section on Second Limiting Current).

Assuming the values of $\bar{i}_o/i_L$ to be about 0.5 for the experimental results, the exchange current per unit volume of electrode is about 0.9 amps/cm^3. Parsons (13) gives the exchange current for this reaction as 6 m amps/sq cm (with a cathodic αn_1 value of 0.58, which suggests an anodic αn_1 of 0.42) on platinum, at 0.015 N in 2N H_2SO_4. Assuming the same exchange current applies here and correcting for the difference in concentration, the effective specific area of the electrode would be (0.9/2)(1000) = 450 sq cm per cm^3, which is a reasonable figure. Assuming Δ/b to be about 5, b about 0.052 volts, then for i_L = 185 m amps/sq cm, ρ is equal to 14 ohm. cm. The specific resistance of 1 N H_2SO_4 is about 2.6 ohm. cm, therefore

$$q/\epsilon = \rho/\rho^1 \simeq 5.3$$

5.3 is a very reasonable value since an electrode of, for example, 30% porosity with a tortuosity factor of $\sqrt{2}$ would give $q/\epsilon = 4.7$.

EXPERIMENTAL RESULTS

The results reported here have been only recently obtained and insufficient work has been done to present a complete picture. However, some interesting results on half cells can be reported which show the limits of the range of application of the theory presented above. The data has been obtained using a galvanostatic technique, with a porous electrode mounted in a lucite holder (the circuit and apparatus will be described in a later report).

To test whether the theory could explain, in a qualitative manner, results for dissolved fuels such as methanol, a porous electrode made of platinum black was used. The use of this catalytic material made it possible to reach the limiting currents at voltages before the oxygen evolution potential. A known weight of platinum black was compressed between two 80 mesh screens of bright platinum. For the thicker electrodes made with a greater weight of platinum black, a third screen was used in the centre of the electrode. The electrode was clamped in a lucite holder to give compression of the powder. The ohmic resistance through the electrode material was found to be negligible. A fritted glass disc was used at the entrance face of the electrode to provide a rigid backing and to ensure even flow distribution. A counter electrode of platinum screen was mounted in the lucite tube, in line with the porous electrode. The cell was run vertically, with the reactant dissolved in the electrolyte entering at the bottom, flowing through the fritted disc and the platinum black electrode, up past the counter-electrode (at which hydrogen was evolved) and out to a collecter for flow rate measurement. Evolved gases were taken off from the top of the cell. The voltage between the electrode and the entering electrolyte was measured versus a saturated calomel electrode. The electrode-electrolyte voltage at the exit face was also measured, versus the saturated calomel electrode, by extrapolation to the electode face of measurements at two known positions downstream.

Blank measurements made without a dissolved reactant showed negligible current densities between hydrogen evolution potentials and oxygen evolution potentials. Some typical results using dissolved fuel are shown in Figures 10 to 13. All tests were made at room temperature. The broken lines represent the inlet voltage and the solid lines the exit voltage, where the latter is the curve which shows the full voltage loss at the electrode (see later discussion of Figure 15). In general the curves were very stable and providing the voltage was not taken too near to oxygen evolution, it was usually possible to go up and down the curve with negligible hysteresis.

It is obvious that the results for this type of electrode cannot be completely explained by the simple theory developed previously. In general, the limiting currents obtained at the larger flow rates were less than those expected from the amount of reactant being forced through the electrode. A discussion of the reasons

for this apparent anomaly is given in the next section.

SECOND LIMITING CURRENT

A study of the results in Figures 10 and 11 show that at low rates of flow, the limiting current obtained was higher than the expected value. This is partly due to external back diffusion of unreacted fuel present in the exit volume of the cell. In time, the flow of fuel-depleted electrolyte will flush out the exit compartment, but at low rates of flow this is a slow process. In later tests on a slow flow rate we kept an electrode near the limiting current for over an hour and a slow drift of the limiting current to the expected value was observed. (This was a tedious process since it required constant adjustment of the current to prevent the potential going to oxygen evolution.) Diffusion from the entrance volume was negligible due to the sintered glass disc at the entrance, and back diffusion could have been greatly decreased by using another disc at the electrode exit. However, this could have prevented the use of a simple extrapolation method to obtain the exit face polarization. At higher flow rates and limiting currents, the back diffusion is proportionately less and the flushing of the exit dead space proportionately faster. It was found that at a flow rate of about 0.4 cm/min the back diffusion effect was almost negligible.

Figures 10 and 11 also show that at high flow rates the limiting current is less than that expected. There are at least three possible reasons for this. Firstly, radial mass transport hindrance across the pores of the electrode might be significant. Secondly, the rate of chemisorption of the fuel might be rate limiting, in which case a chemisorption limiting current is obtained when the fractional surface coverage θ tends to zero all over the electrode (7). Thirdly, the electrochemical discharge may be preceded by a dissociation in the bulk of the pore electrolyte and the limiting current would then be determined by a limiting rate of the predissociation.

Considering the first possibility, that of radial mass transport, the problem can be solved with sufficient accuracy by considering the mass transfer analogy to radial heat transfer in laminar flow systems. The solution for laminar flow, for a fixed concentration at the wall and for fully developed velocity and concentration profiles, is given by (14)

$$Nu = hD/k = 3.66$$

$$\text{rate per unit area} = h(R_m - R_w) \qquad (23)$$

D is the pore diameter; k is the mass transfer coefficient, which is the diffusion coefficient of the reactant in this case; R_m is the mass flow mean concentration of reactant and R_w is the concentration at the wall of the pore. The assumption of negligible entrance effects, and fully developed flow, is probably reasonably good because of the very low Reynold's numbers of flow in fine pores. A limiting current is clearly reached when $R_w = 0$ at all points along the wall of the pore. Let A be the specific geometric area of the walls of pores, in cm^2 of area per cm^3 of electrode (note that A does not necessarily equal S). Then the differential current density in an element dx at the condition where $R_w = 0$ is

$$di = nF\ 3.66(k/D)AR_m dx \qquad (24)$$

At the same time

$$di = nFv\ dR$$

$$i = nFv(R_i - R_m)$$

$$i_{Ll} = nFvR_i$$

Therefore,

$$R_m = (i_{L1} - i)/nFv$$

and

$$\int_0^{i_{L2}} (1/(i_{L1} - i))di = 3.66(Ak/Dv) \int_0^L dx$$

or

$$i_{L2}/i_{L1} = 1 - e^{-3.66(AkL/vD)} \quad . \tag{25}$$

Thus the ratio of the observed limiting current i_{L2} to that of the expected limiting current i_{L1} is given by equation 25, where A/D is an unknown factor. An estimate of the ratio of limiting currents can be made by taking L as 0.1 cm, k as 10^{-5} cm^2/sec, v as 1 cm/sec, A as 500 cm^2/cm^3 and D as 10 microns. The exponent of the exponential term is then approximately -20 and the radial mass transport effect would be negligible. However, a 10 fold decrease in the magnitude of exponent, given for example by A = 250 cm^2/cm^3 and D = 50 microns, would give a significant effect.

The second possibility, that of a chemisorption rate limitation can be analyzed by assuming that the limiting rate of chemisorption is given by,

$$\text{rate per unit area} = k_1R, \text{ gm moles/cm}^2\text{sec.} \tag{26}$$

This follows from a chemisorption rate equation when $\theta \to 0$, $1 - \theta \to 1$. k_1 is the rate constant. Equation 24 is now replaced by

$$di = nFk_1SR\ dx.$$

The treatment then follows as before giving

$$i_{L2}/i_{L1} = 1 - e^{-(Sk_1L/v)}$$

The third possibility, of a dissociation before discharge, is similarly handled by assuming a dissociation rate of

$$\text{rate per unit volume} = k_2R$$

A limiting rate is obtained when the reaction is irreversible and the product of reaction is removed, by electrochemical reaction, as fast as it is formed. Then the differential current density is given by

$$di = nFk_2R\epsilon\ dx$$

and, as before,

$$i_{L2}/i_{L1} = 1 - e^{-(k_2\epsilon L/v)} \tag{29}$$

Thus the three possibilities all give rise to a form

$$i_{L2}/i_{L1} = 1 - e^{-(JL/v)} \tag{30}$$

where the exponent includes L/v in all cases, but J has a different physical meaning for the different cases.

If equation 27 or 29 applied it might be expected that different fuels would give different values of J, whereas if equation 25, that for radial mass transport, applied then J would be nearly constant for different fuels.

DISCUSSION OF RESULTS

Table 2 shows the value of J calculated for a number of different tests. L was determined from the weight of platinum black used in constructing the electrode, from the relation 100 mg per $cm^2 \approx 1$ mm of thickness. For methanol and potassium formate the value of J was approximately constant, with a mean value of 4.8. When it is considered that the electrodes are pressed powder and can vary between one pressing and another, it must be concluded that J is constant within the reproducibility of the system. No significant difference was present between methanol in acid or methanol in alkali, or between these and potassium formate in alkali. This

TABLE 2. Values of J for Various Systems

Fuel	n, Electrons Used to Calculate i_{L1}	Molar Concentration of Fuel	Electrolyte	mg/cm^2 of pt. Black	L cm	v cm/min	J
Methanol	6	0.05	4MKOH	230	0.23	1.0	4.3
		0.1	4MKOH	200	0.20	0.57	6.8
		0.1	$3MH_2SO_4$	80	0.08	0.4	4.3
		0.1	$3MH_2SO_4$	80	0.08	1.0	5.1
Potassium Formate	2	0.04	4MKOH	230	0.23	1.0	3.9
		0.05	4MKOH	230	0.23	2.03	4.3
		0.2	4MKOH	230	0.23	0.37	5.4
		0.2	4MKOH	230	0.23	1.0	4.0
						Mean	4.8
Potassium Borohydride	8	0.02	4MKOH	80	0.08	2.5	28
		0.02	4MKOH	80	0.08	4.0	33
Hydrazine	4	0.02	4MKOH	80	0.08	1.37	33
		0.02	4MKOH	80	0.08	2.0	37
		0.1	4MKOH	80	0.08	1.0	43
						Mean	35

is evidence that the effect is one of radial mass transfer. However, the results from hydrazine (see below) suggest that if radial mass hindrance is present then gas evolution reduces this effect. Gas evolution was observed with methanol in acid electrolyte. For potassium borohydride and hydrazine, on the other hand, J was again reasonably constant but with a mean value of 35. Bigger J means less departure from the expected limiting current and would be due to an increased mass transport factor, increased rate of chemisorption or increased rate of predissociation. The hydrazine reaction is;

$$N_2H_4 + 4OH' \rightarrow N_2 + 4H_2O + 4e \ .$$

Vigorous gas evolution from the test electrode was observed. Thus for this type of electrode, the nitrogen evolved within the electrode may increase the effective radial mass transport factor; it does not appear to block the electrode. A blockage of the electrode by trapped gas bubbles would be expected to reduce the effective internal area of the electrode, leading to higher polarization and a reduction in J. Blockage does not seem to occur and the reason may be that since reaction is concentrated towards the exit face, the small bubbles produced by the reaction may reach the exit face, by vertical travel, before they grow very large.

Decomposition of the borohydride to produce H_2 was noted at open circuit conditions. Therefore, some prior decomposition reaction may be postulated,

$$BH_4' + 2H_2O \xrightarrow{Pt} BO_2' + 4H_2 \ .$$

However, the released hydrogen was readily used when appreciable currents were drawn, giving an over-all reaction,

$$BH_4' + 8\ OH' \rightarrow BO_2' + 6H_2O + 8e \ .$$

Certainly, some of the hydrogen released to the surface from the borohydride will never be released as gas under load, since surface hydrogen will be discharged electrochemically. However, it is possible that enough is released and later reused to cause increased radial mass transport, comparable to that observed by hydrazine.

The analysis of J factors given above show that, at least for the platinum powder electrode, the assumption of a negligible radial mass transfer effect may not be valid. Alternatively, a slow chemisorption or dissociation may be present. Although we have not completed the inclusion of these effects in a more comprehensive treatment, it is reasonable to suppose that the voltage-current curves will fit into three categories. Case 1 would be where JL/v is large, the interfering effect is small and the curves correspond to the basic theory. For a one electron rate controlling step at room temperature, the voltage change between $i/i_L = 0.1$ and $i/i_L = 0.9$, for the center of the η_o, η band, is about 0.15 volts. Case 2 would be for a moderate value of JL/v, such that $i_{L2} \approx i_{L1}$, but a considerable effect on the shape of the curve is present. The effect will be to increase the general slope of the voltage-current curves, especially near the limiting current. Case 3 is for a small value of JL/v, which gives a greatly reduced limiting current. At low currents the curves will be nearly the same, but the greater the effect of JL/v then the more gradually will the curves approach the limiting current, the slopes will be greater, and the sharp bend-over near the limiting current for the η_o line will be replaced by a gradual approach. Case 2 behaviour can be seen in Figure 11, the results for potassium formate, where the general slope of the curves is greater than expected, even when the limiting current is close to the theoretical value. Figure 10, the results for methanol in basic solution, also shows this general behaviour but the increase in slope is greater than for the formate case. This is almost certainly due to two steps of comparable rate being involved. Other results we have obtained show that formaldehyde is more rapidly oxidized than methanol or formate, therefore the over-all methanol curve is composed

of,

$$\text{methanol} \xrightarrow{\text{slow}} \text{formaldehyde} \xrightarrow{\text{fast}} \text{formate} \xrightarrow{\text{slow}} \text{carbonate}.$$

If the formate oxidation were much slower than the methanol, two waves in the voltage-current plot would be observed. However, since they are of comparable rate, methanol is reacted to give appreciable concentrations of formate in the electrode, which then further reacts as the voltage increases. The two waves fuze into one long curve.

The analysis of J factors given above indicate that the hydrazine and borohydride reactions are less influenced by the effect. Therefore, it is possible that results for a high value of L/v for these systems may approach the expected values for the simple theory. (It is not possible to use too low flow rates, since back diffusion then becomes appreciable.) Figure 14 shows a comparison of experimental results with computed results for hydrazine, assuming a value of Δ/b of 10, $\alpha n = 1/2$, and a value of $\bar{I}_o/i_L$ of 10^{-3}, based on a theoretical open circuit potential of 1.40 volts (v. saturated calomel). The values were selected from the difference in entrance and exit polarizations and from the position of the curves along the voltage scale. It can be seen that the shapes of the experimental curves are in fair agreement with theory up to values of i/i_L of about 0.7, after which they show steeper slopes and a less abrupt change to the limiting current. Thus, the J factor effect comes into play at the higher current densities, in the expected manner. The observed open circuit potential is considerably more positive than theoretical but this is to be expected since, as the voltage is past the hydrogen evolution potential, a mixed potential will result. Calculation of ϵ/q in the same manner as before gives a value of about 1/9, which is reasonable.

The results shown in Figures 10 to 13 were deliberately taken at low concentrations and flow rates, so that the limiting currents could be reached without heating effects. At concentrations of several moles/litre, and high flow rates, the limiting current densities became so great that heating occurred on the passage of the electrolyte through the electrode. Under these conditions it was possible to obtain current densities of two or three amps/cm^2 at voltages well below the point of oxygen evolution but, in the design of cell used, the ohmic heating at this high current caused instability due to boiling of the electrolyte.

The voltage in a fuel cell consisting of two flow-through electrodes using fuel and oxidant is illustrated in Figure 15. Line ab represents the voltage change between the electrode potential at a and the electrolyte at b, at ideal zero current conditions. cd is the voltage change from the electrolyte to the cathode under these conditions. Under load, eb is the loss of voltage, η_{o1}, due to initial activation polarization on the fuel electrode, while η_1 is the total polarization through the electrode. The line fghi represents the ohmic voltage gradients through the free electrolyte, gh being that across a separator. ijk is the equivalent cathode voltage curve to gef for the anode. The terminal voltage is now V, where $V = E_o - (\eta_1 + \eta_r + \eta_2)$. The results presented in Figures 10 to 13 show only η_1 values versus current density for the given fuels.

CONCLUSIONS

The theory developed for the combined effects of activation, concentration and ohmic polarization at porous flow-through electrodes is likely to apply for simple redox systems and electrodes of small pore diameter. In studies of this kind of electrode it is essential to make measurements of entering and exit voltage in order to obtain a complete picture of the process. Results using methanol, formaldehyde, potassium formate, hydrazine and sodium hydroboride at non-consolidated electrodes of platinum black show that further factors are involved. These factors may include more complex forms of the electrochemical discharge equation, involving a bulk predissociation or chemisorption step, or a radial mass transfer hindrance.

Further work is planned on the theory of such systems. It is also planned to test the basic equation for simple redox systems and fine-pore consolidated electrodes.

Using platinum black flow-through electrodes at room temperature it was found that, at appropriate flow rates, methanol could be completely oxidized to carbonate in alkaline solution or CO_2 in acid solution. Tests on formaldehyde and potassium formate in basic solution showed that the formaldehyde is relatively rapidly oxidized compared to methanol, while formate is only slightly more readily oxidized. It was not possible to tell whether the chemisorption of methanol or the initial breakdown of methanol to formaldehyde was the first slow step. On the same type of electrode, potassium borohydride could be completely utilized giving eight electrons per molecule and hydrazine could be utilized to N_2, giving four electrons per molecule. The evolution of gas did not hinder the performance of the electrode.

REFERENCES

(1) Posner, A. M., Fuel 34, 330 (1955).

(2) General Electric Company, Aircraft Accessory Turbine Dept., "Research on Low Temperature Fuel Cell Systems", Progress Report No. 8, Contract No. DA-44-009-ENG-4771, U. S. Army E.R.D.L., Ft. Belvoir, Virginia. ASTIA No. AD 243 474; (1960).

(3) Austin, L. G., "Fuel Cells" in "New Techniques for Energy Conversion", Ed. S. N. Levine, Dover Pub. Inc.

(4) Guillou, M., "Repartitions couplees du potential et des concentrations dans les cellules electrochemique." Thesis presented to Faculte des Science de p'Universite de Paris, 1963. Also private communications from R. Buvet, Electricite de France.

(5) Lockheed Missiles and Space Company, "Basic Studies on Fuel Cell Systems", Quarterly Reports No. III and IV, Contract NOW60-0738-d, Bureau of Naval Weapons. ASTIA Nos. AD 273 702, AD 278 353; (Nov. 1961 to May 1962).

(6) Monsanto Research Corporation, "Compact Power Fuel Cell", Report ASD-TDR-62-42, Contract AF33(616)-7735, Flight Accessories Lab., Wright Patterson Air Force Base. ASTIA No. AD 282 862; (June 1962).

(7) Austin, L. G., "A Discussion of Some Aspects of Electrode Kinetics Relevant to Fuel Cell Studies", Report No. 1, Contract DA49-186-502-ORD-917, Diamond Fuze Laboratories, Washington, D. C. (June 1962).

"Electrode Kinetics and Fuel Cells", Proc. Inst. Elec. and Electronic Engineers, 51, 820 (1963).

(8) Perskaya, R. M. and Zaidenman, I. A., Proc. Acad. Science U.S.S.R., Physical Chemistry Section, 115, 513 (1957).

(9) Bond, A. P. and Singman, D., "Electrode Kinetics of Oxidation - Reduction Couples", Diamond Ordnance Fuze Laboratories, Washington 25, D.C. (1960).

(10) Carman, P. C., "Flow of Gases Through Porous Media", Academic Press, Inc., New York, 1956.

(11) Austin, L. G., "Polarization of Porous Flow-Through Electrodes, Report No. 2, Contract DA49-186-502-ORD-917, Diamond Ordnance Fuze Laboratories, Washington 25, D. C. (Sept. 1962).

(12) Vetter, K. J., "Elektrochemische Kinetik", Springer-Verlag, Berlin, p. 380, 1961.

(13) Parsons, R., "Handbook of Electrochemical Constants", Academic Press, Inc., New York, 1959.

(14) Rohsenow, W. M. and Choi, H. Y., "Heat, Mass and Momentum Transfer", Prentice Hall, Inc., New Jersey, p. 141, 1961.

LIST OF NOMENCLATURE

A,	specific geometric area of pore walls.
b	$= RT/\alpha n_1 F$
D,	pore diameter
f	$= \exp(\eta/b) + \gamma\exp(-\eta/b)$
F,	Faraday
i,	current density
i_o,	true exchange current density
$\bar{i}_o$,	$= i_o SL$, apparent exchange current density for the electrode
i_L,	limiting current density
i_{L1}	$= nFvR_i$, expected limiting current density
i_{L2}	obtained limiting current density
J,	defined by equations 28, 30, 32, 33
k,	mass transfer coefficient of reactant, cm^2/sec
k_1,	specific rate constant for chemisorption
k_2,	rate constant for dissociation
L,	thickness of electrode, cm
M,	number of increments into which L is divided
n,	number of electrons involved in the reaction
n_1,	number of electrons involved in the rate controlling step
N	N'th increment between 0 and M
Nu	Nusselt number
P,	concentration (activity) of product at distance x in the electrode
P_i,	initial value of P, at $x = 0$
q,	tortuosity factor for conduction in electrolyte in the pores of the electrode
Q	$= \exp(\eta/b) - \exp(-\eta/b)$
R,	concentration (activity) of reactant at distance x in the electrode
R_i,	initial value R, at $x = 0$
RT,	gas constant times absolute temperature
S,	effective specific area of electrode interior, cm^2/cm^3
v,	velocity of flow of feed, cm/sec
x,	distance into electrode from entrance face
$\bar{x}$	$= x/b$
α,	transfer coefficient in the direction of reaction
Δ	$= i_L \rho L$, maximum ohmic polarization
$\bar{\Delta}$	$= \Delta/b$
ϵ,	porosity of the electrode
η,	polarization
$\bar{\eta}$	$= \eta/b$
η^1	$= \eta - \eta_o$
η_o,	polarization at entrance face
η_s,	Polarization with negligible internal ohmic effect
γ,	ratio of inlet reactant concentration to inlet product concentration
ρ_i	effective specific resistance of electrolyte in the pores, ohm.cm
ρ^1,	true specific resistance of the electrolyte

ACKNOWLEDGEMENTS

The work reported here has been performed for the Harry Diamond Laboratories, Washington, D.C. under contract DA49-186-502-ORD-917. Grateful acknowledgement is made to the United States Army Materiel Command for permission to publish the work.

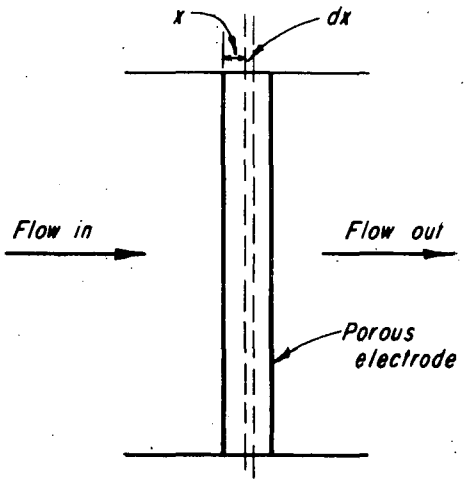

FIGURE 1. Illustration of System Studied.

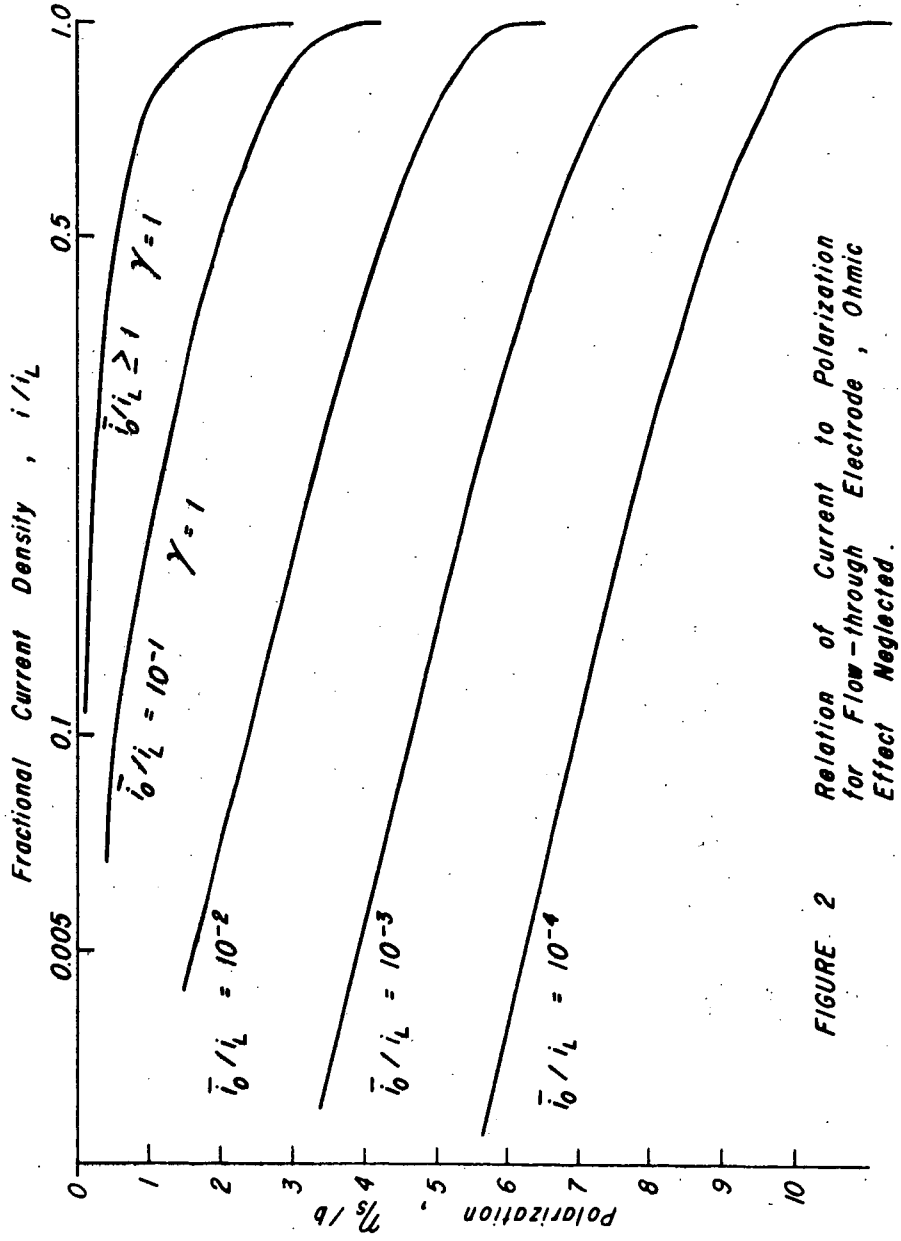

FIGURE 2 Relation of Current to Polarization for Flow-through Electrode, Ohmic Effect Neglected.

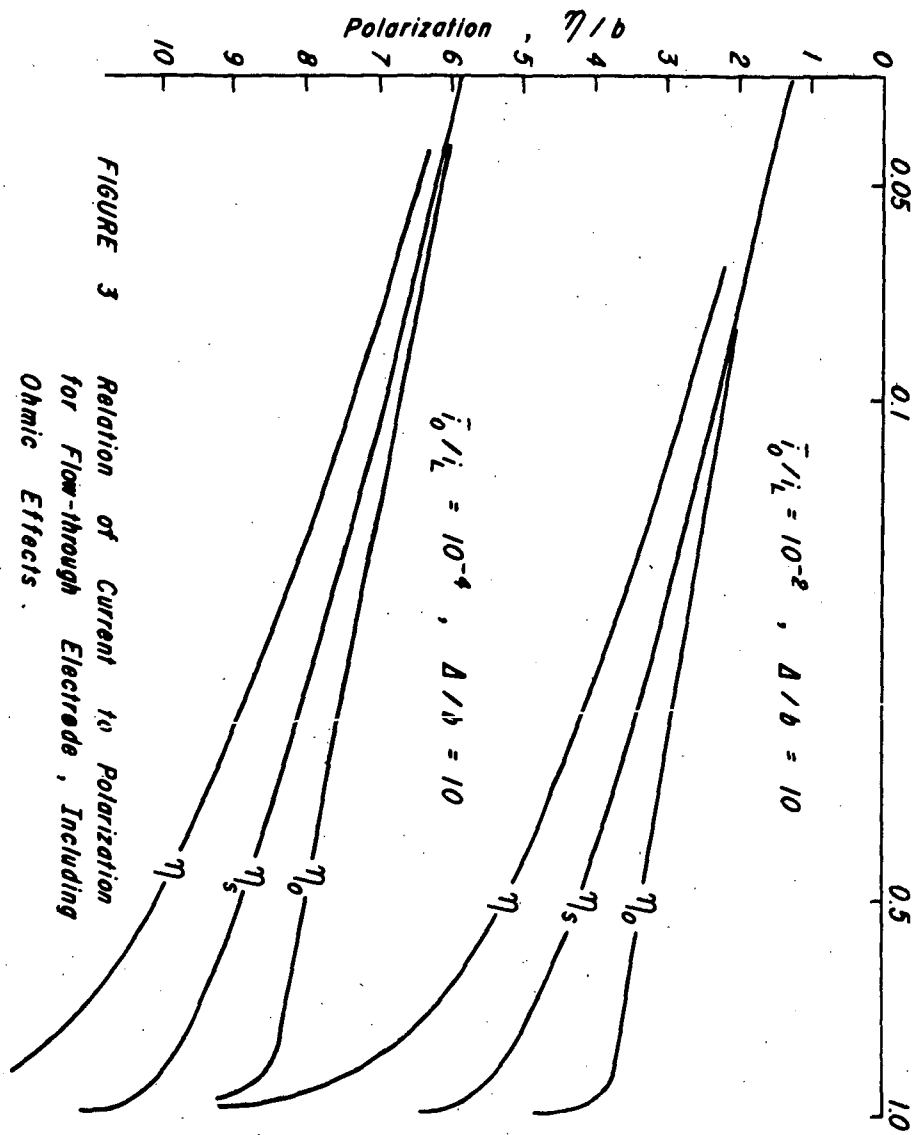

FIGURE 3 Relation of Current to Polarization for Flow-through Electrode, Including Ohmic Effects.

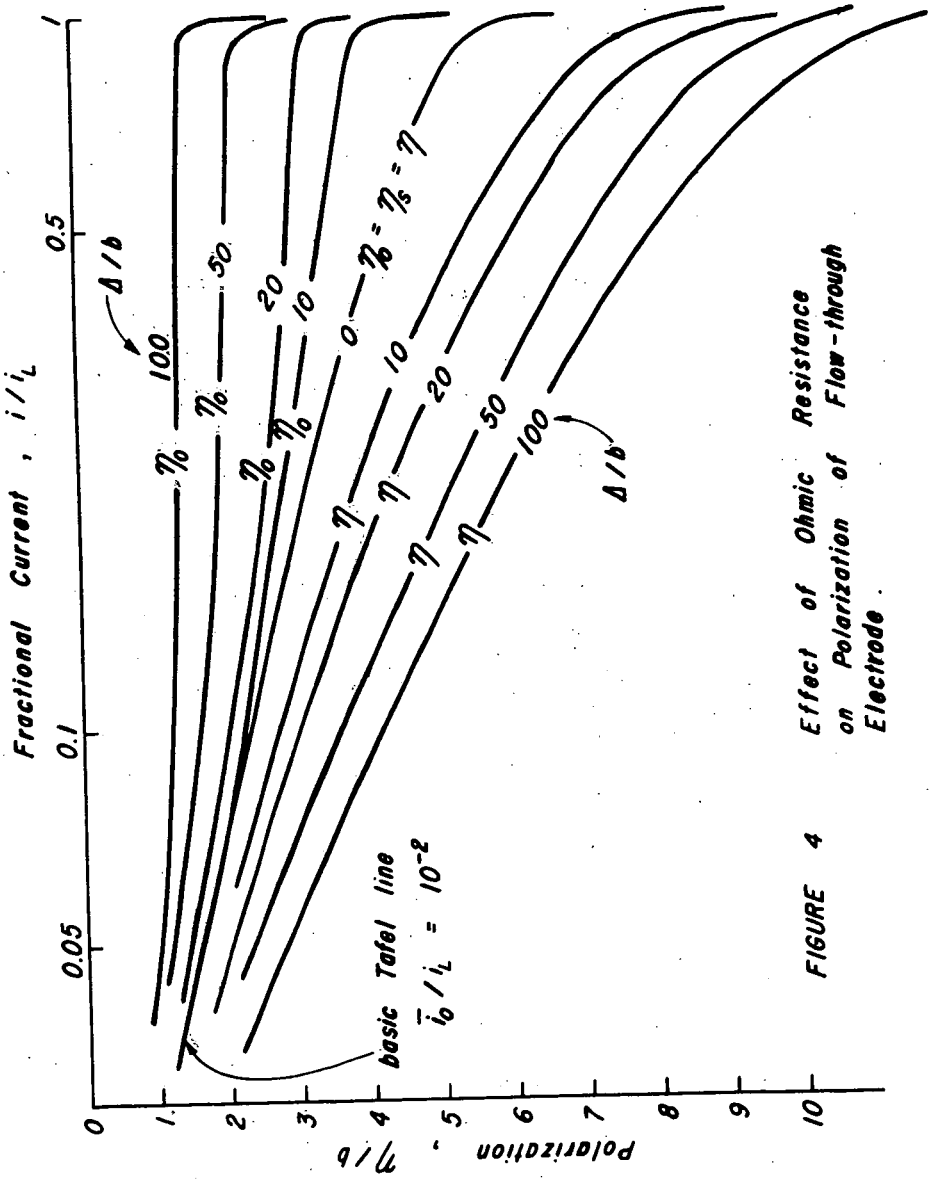

FIGURE 4 Effect of Ohmic Resistance on Polarization of Flow-through Electrode.

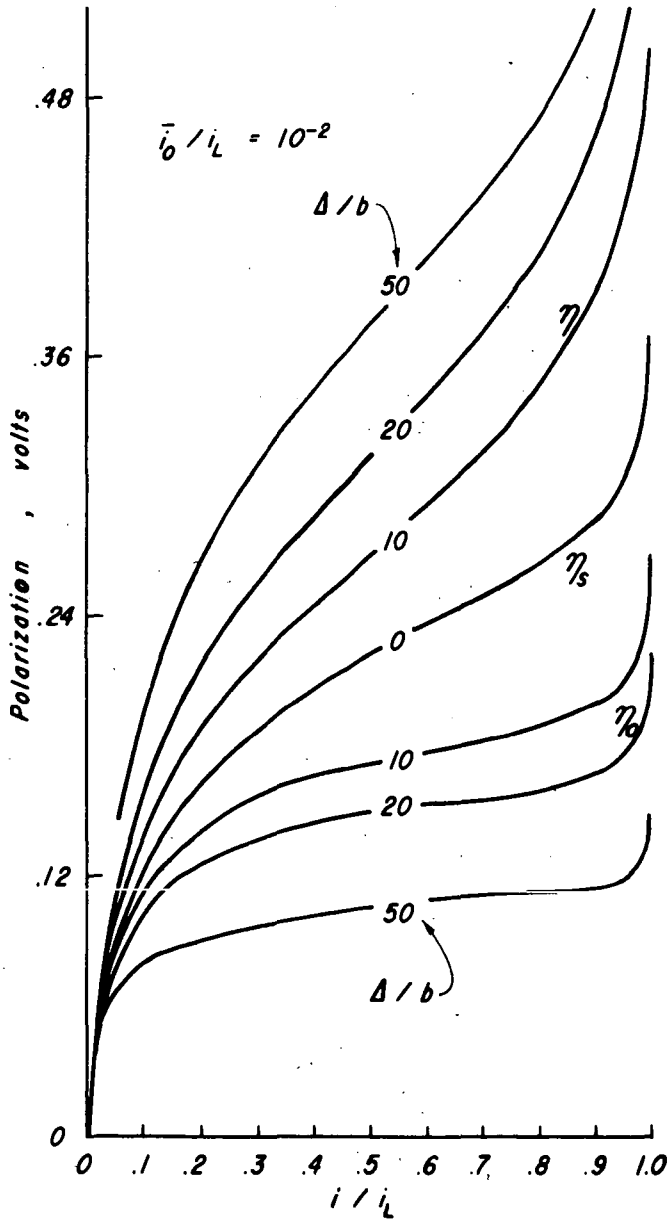

FIGURE 5 Results of Figure 4 for a One Electron Rate Controlling Step , Tafel Coefficient Equal to 0.12volts .

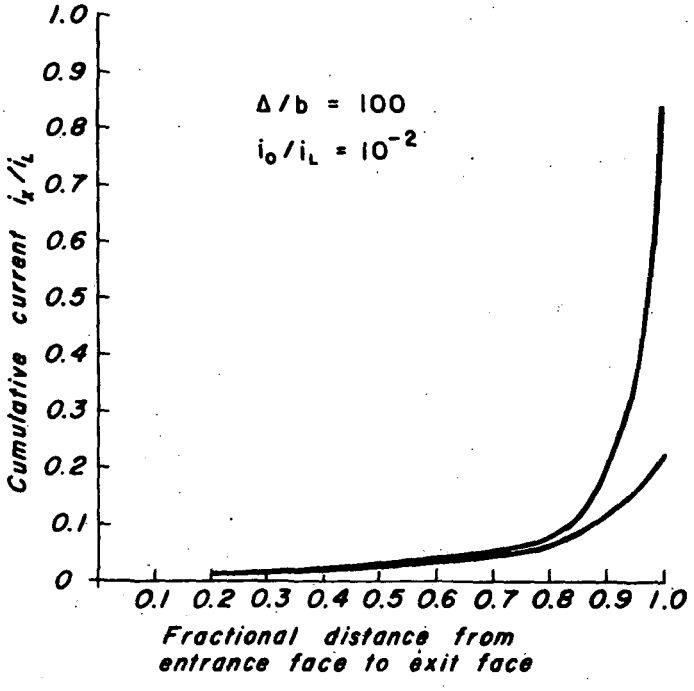

FIGURE 6 *Cumulative reaction through a flow-through electrode.*

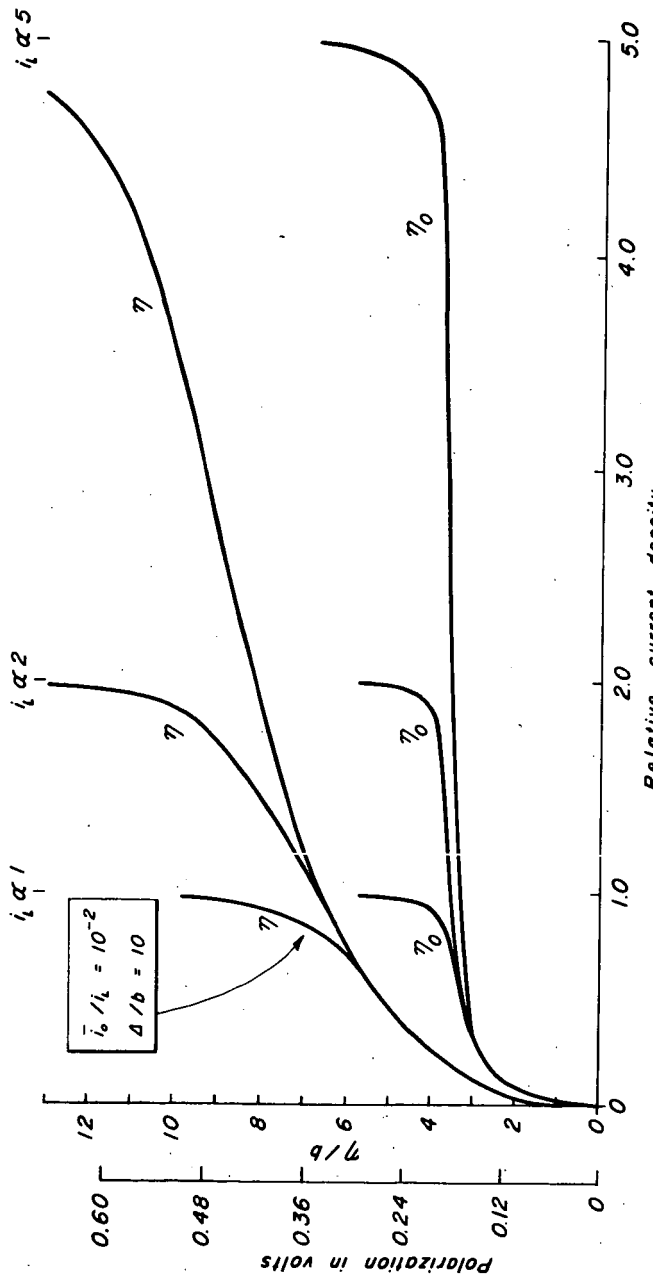

FIGURE 7 Computed Effect of Increasing Flow Rate.

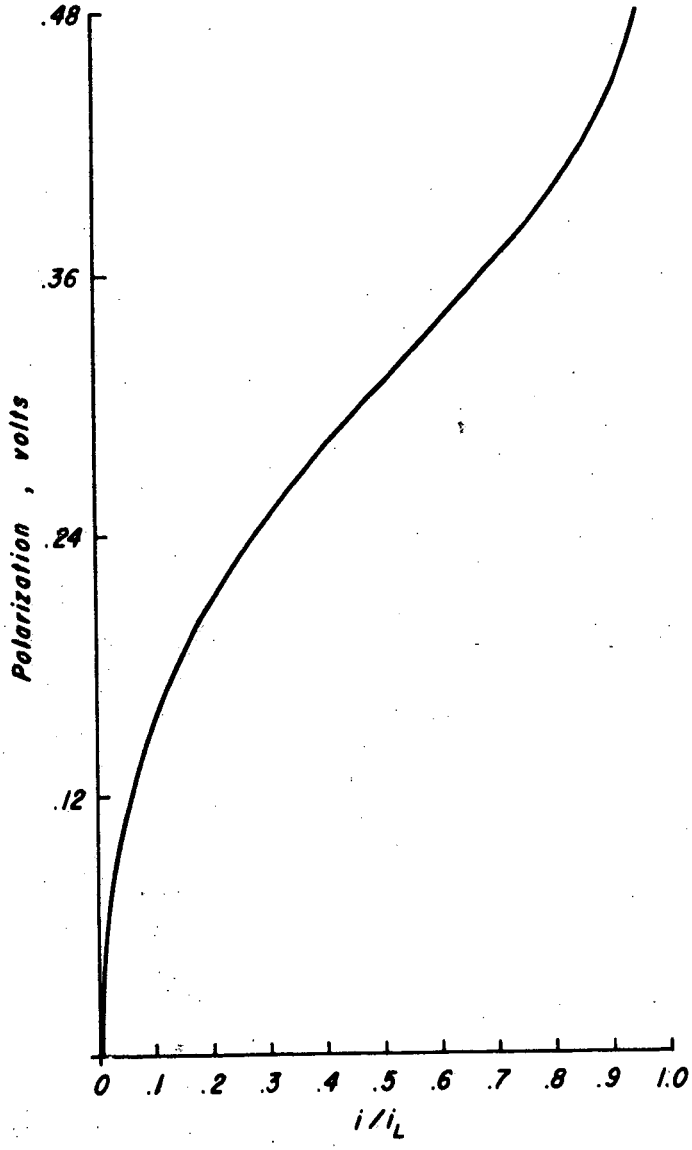

FIGURE 8 . Polarization Curve for $Sn^{2+} \rightarrow Sn^{4+}$, i_L = 80 m amps / cm^2. (see table I)

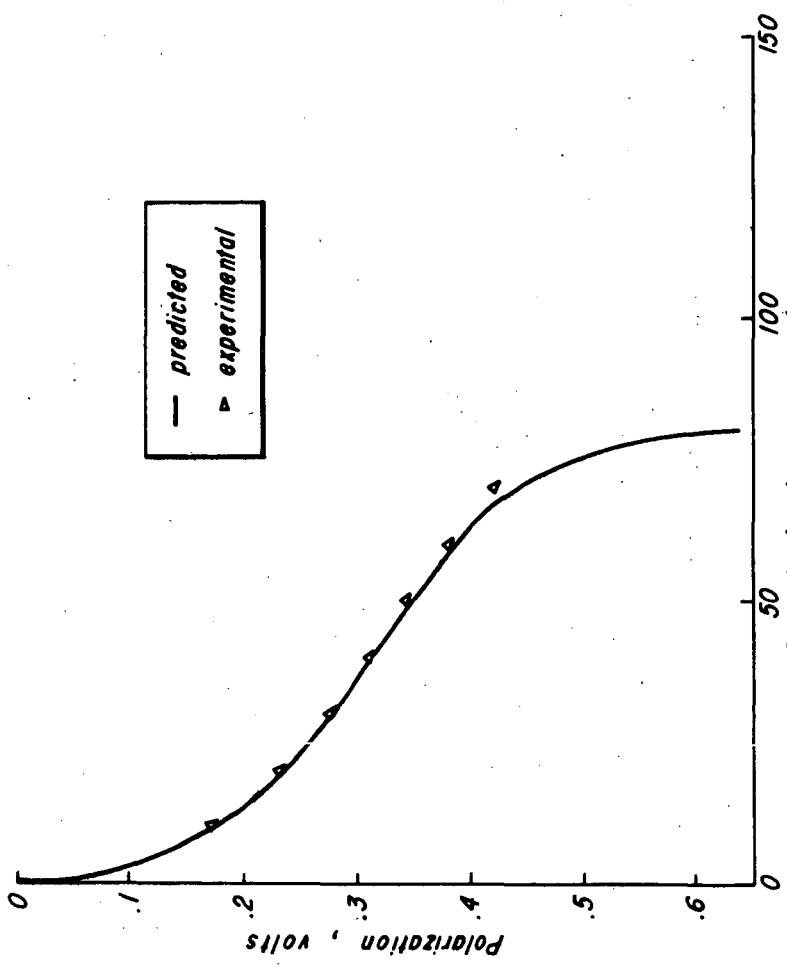

FIGURE 8a Comparison of Computed with Experimental Polarization. (Sn^{2+}/Sn^{4+} couple)

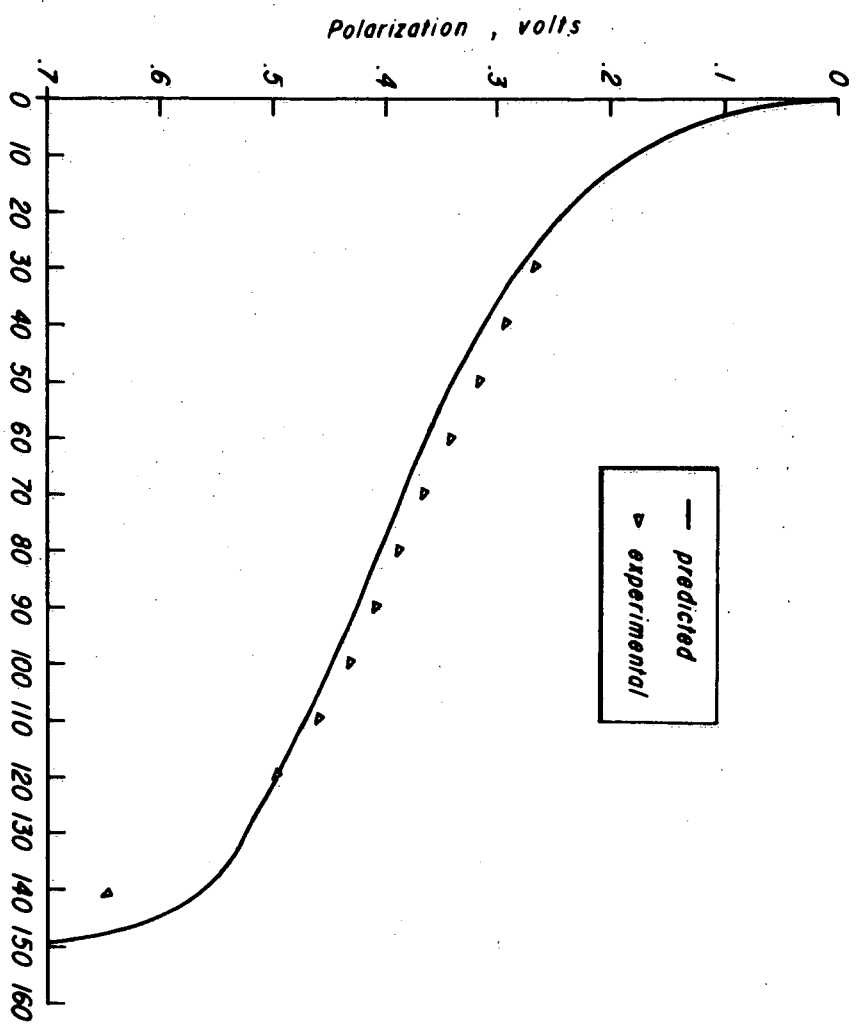

FIGURE 8b Comparison of Computed with Experimental Polarization. (Sn^{2+}-Sn^{4+} couple)

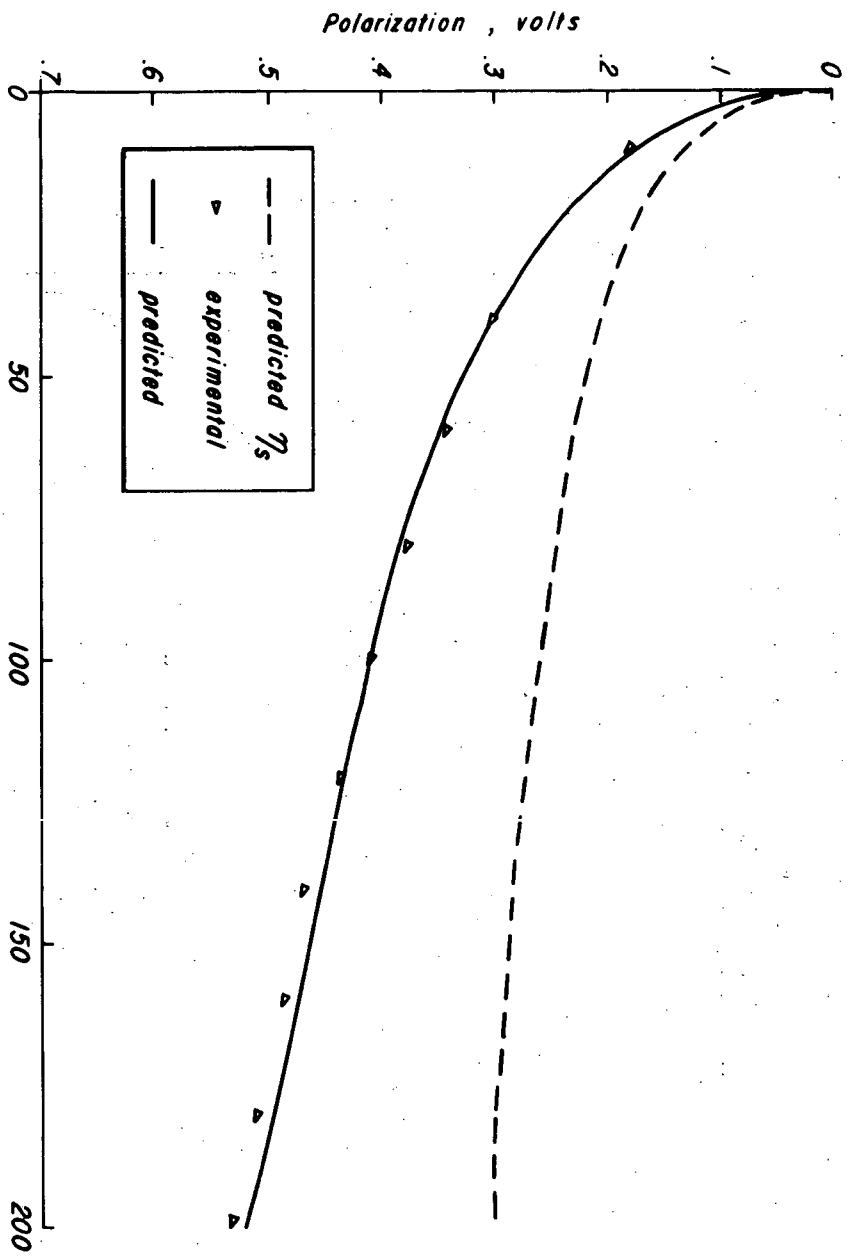

FIGURE 8c Comparison of Computed with Experimental Polarization. (Sn^{2+}-Sn^{4+} couple)

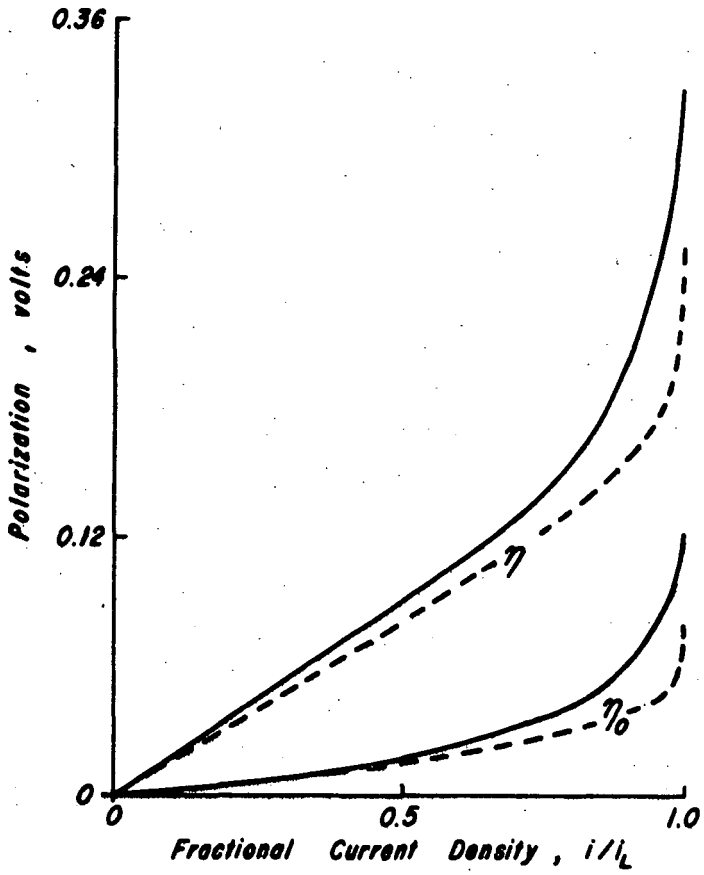

FIGURE 9 — Polarization Curve for $Fe^{2+} \rightarrow Fe^{3+}$, i_L = 185 m amps / cm^2.

-- Computed Polarization for Flow-through Electrode; i_0/i_L = 0.5, Δ/b = 5.

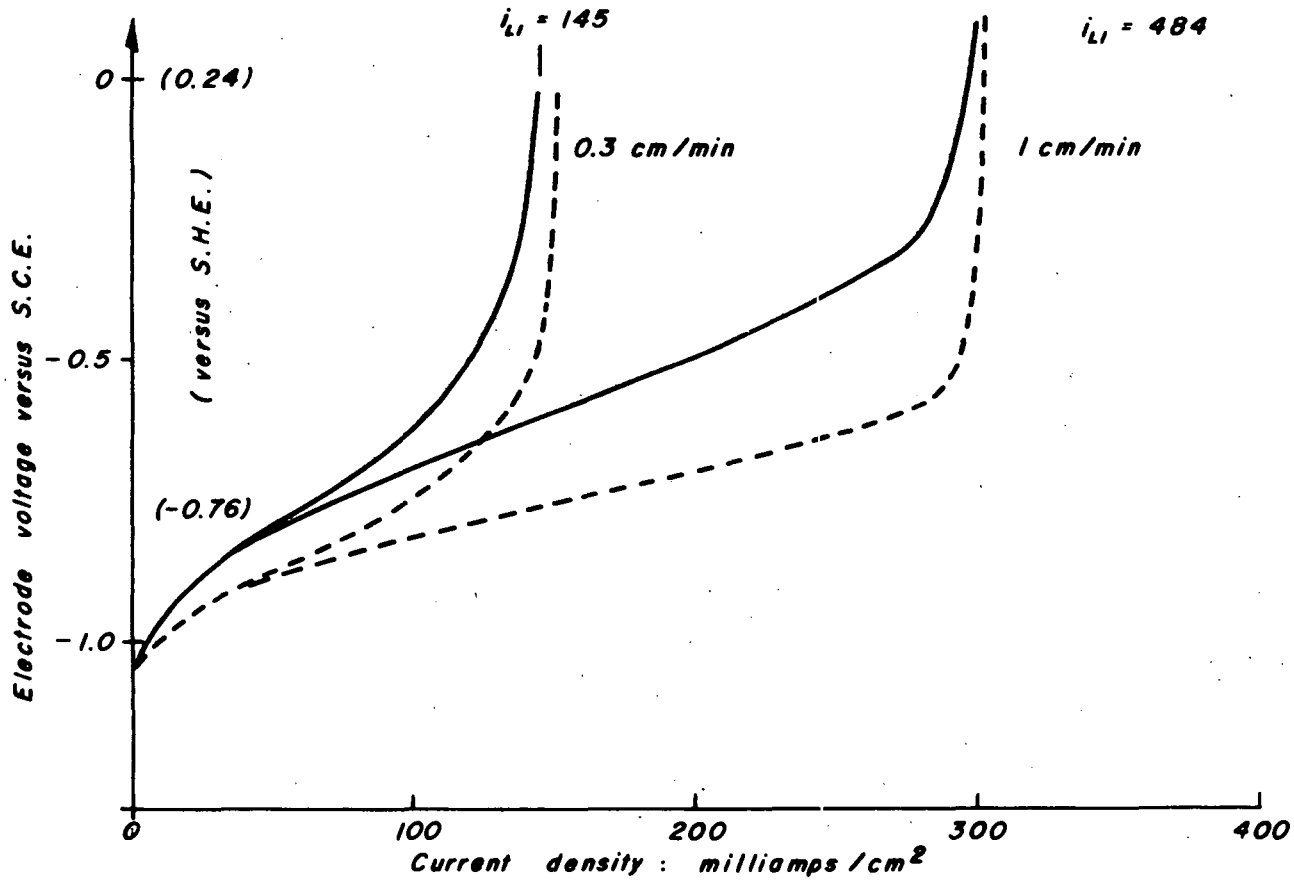

FIGURE 10 Fuel, Methanol 0.05 M ; Electrolyte, 4M KOH ; Electrode, 230 mg/cm² Pt Black.

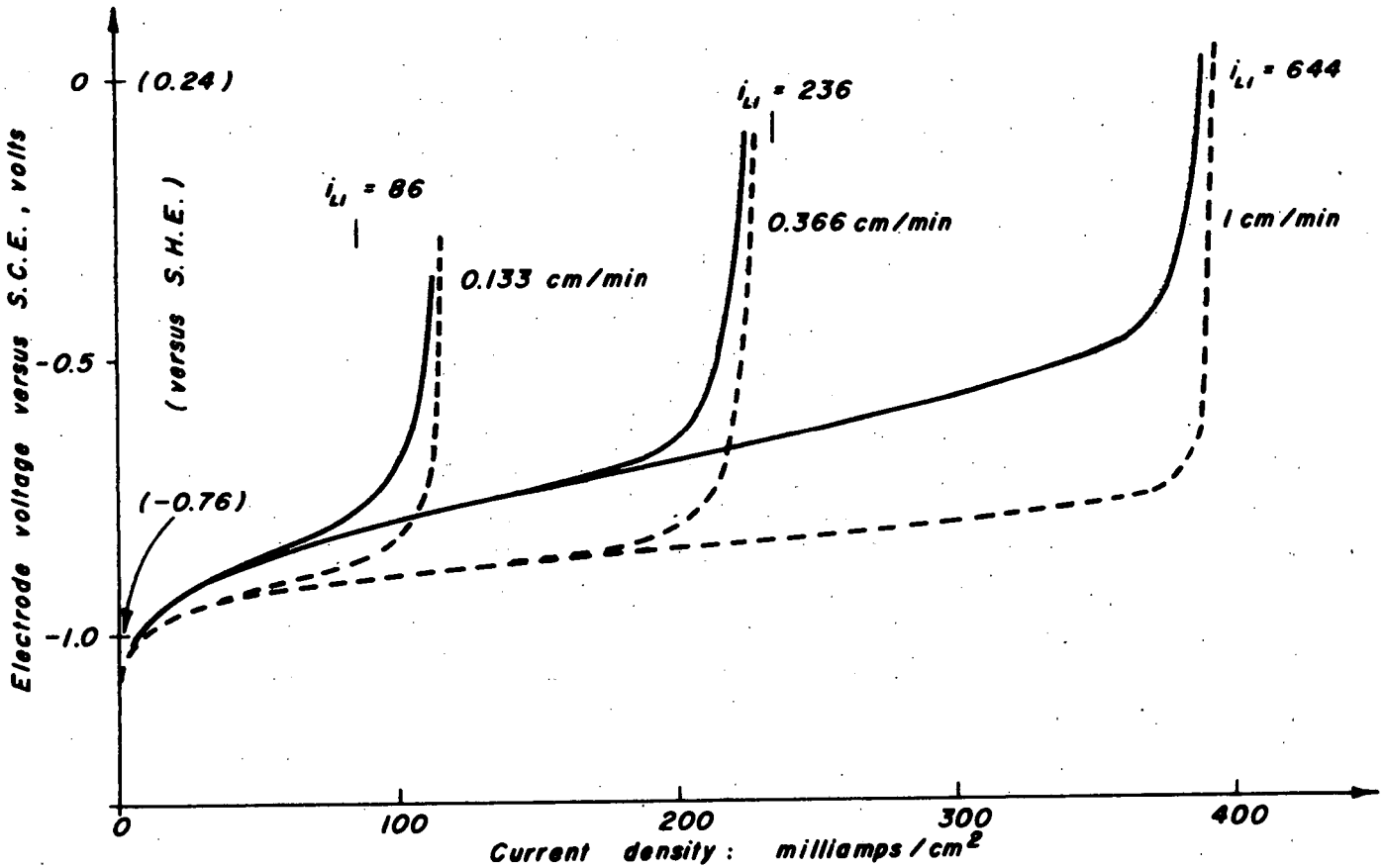

FIGURE 11 Fuel, Potassium Formate 0.2M; Electrolyte, 4M KOH; Electrode, 230 mg/cm^2 Pt Black.

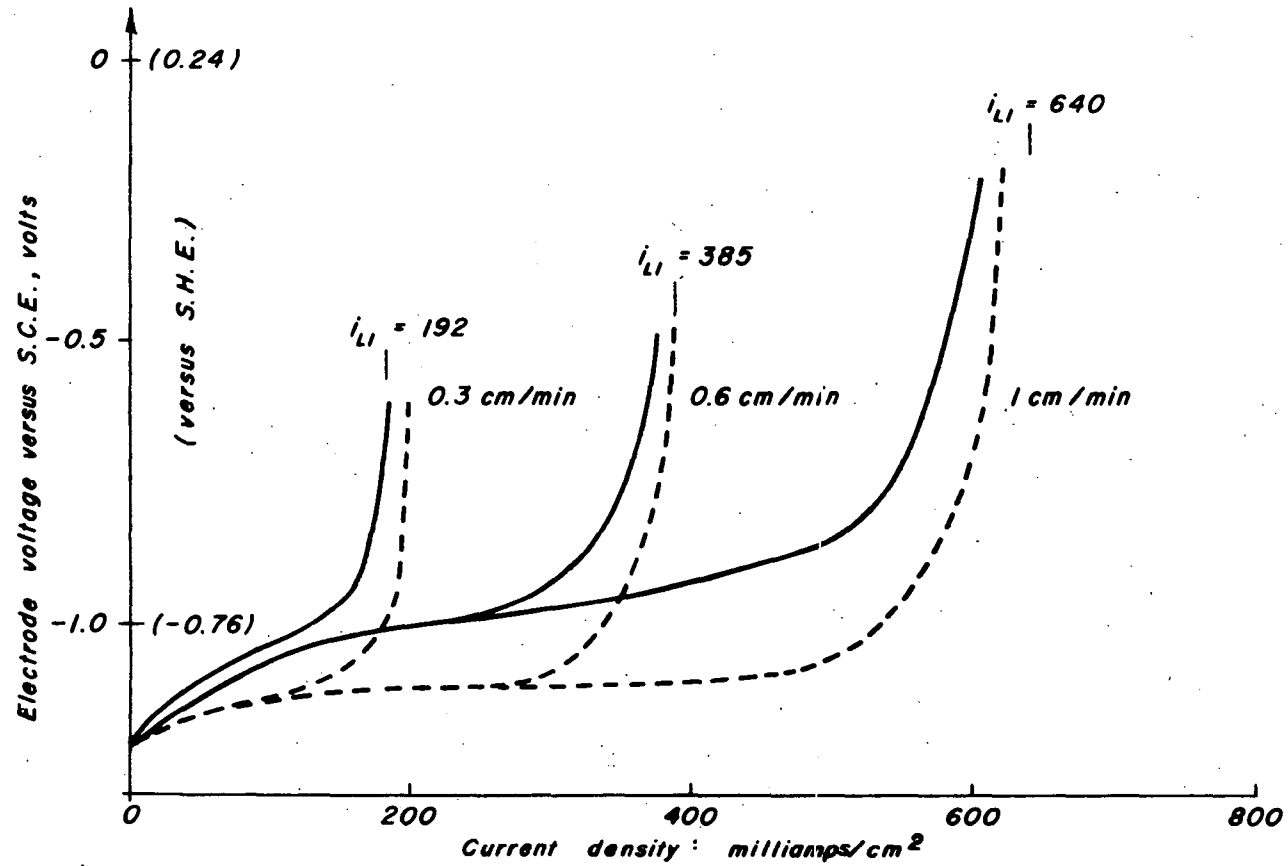

FIGURE 12 Fuel, 0.1M N_2H_4 ; Electrolyte, 4M KOH; Electrode, 80 mg/cm^2 Pt black.

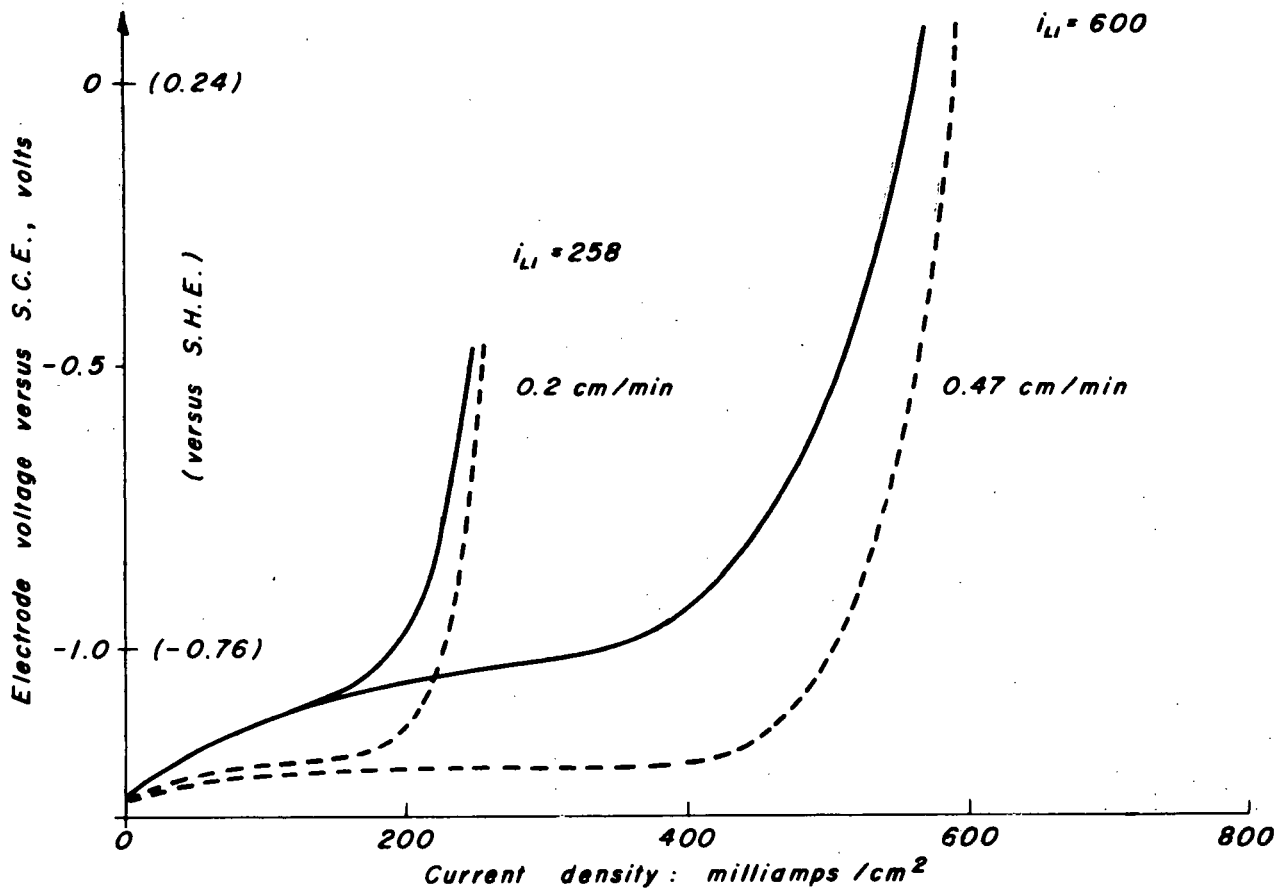

FIGURE 13 Fuel, 0.1M KBH_4 ; Electrolyte, 4M KOH; Electrode, 80 mg/cm² Pt Black.

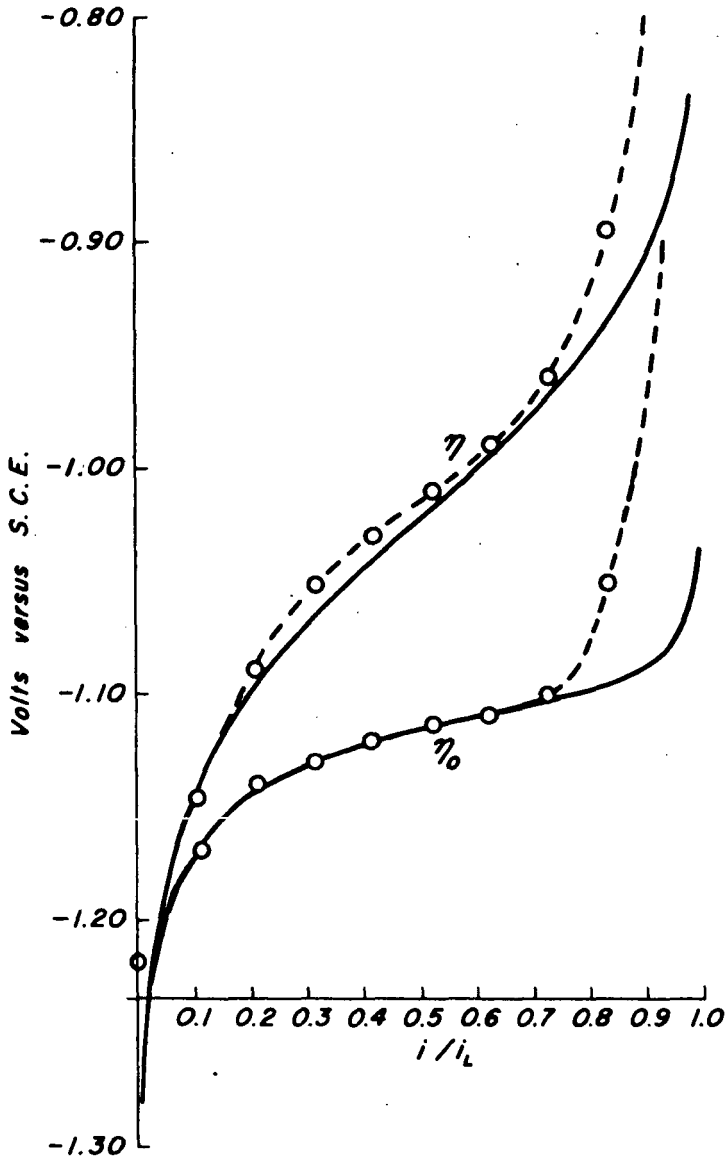

FIGURE 14 — O Experimental values for 0.1M N_2H_4 in 4M KOH, 0.6 cm/min, 80mg/cm^2 Pt black.

— Computed curve for $\Delta/b = 10$, $i_o/i_L = 10^{-3}$

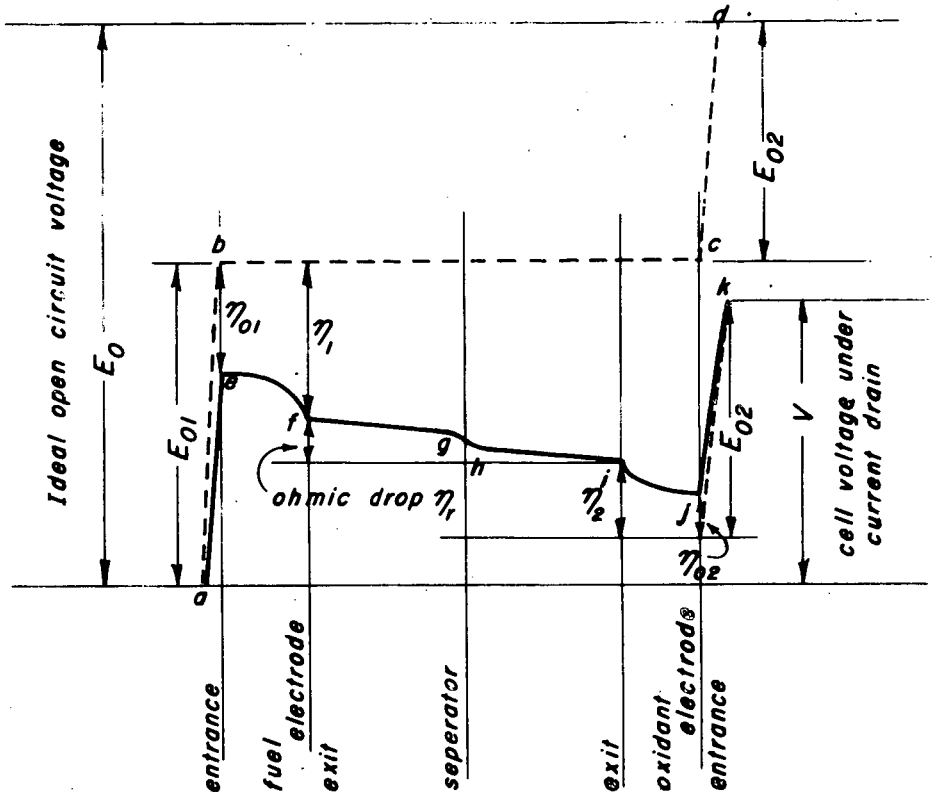

FIGURE 15 Illustration of Voltage Gradients within Cell.